Investigating the pottery firing techniques in western Slovenia during the Late Bronze and Early Iron Ages using FTIR and petrographic analysis

Manca Vinazza[1], Petros Chatzimpaloglou[2]
1 Department of Archaeology, Faculty of Arts, University of Ljubljana, Ljubljana, SI; manca.vinazza@ff.uni-lj.si
2 McDonald Institute for Archaeological Research, University of Cambridge, UK; pc529@cam.ac.uk

ABSTRACT - *This study focuses on the analysis of pottery firing techniques during the Late Bronze and Early Iron Ages in the Karst region of Slovenia. Given the absence of archaeological structures, we adopted an alternative research approach, employing FTIR and ceramic thin-section analysis. The archaeological material underwent study using a model derived from archaeological experiments, which encompassed firing techniques in both pits and pottery kilns. Our research successfully identified that various firing structures were utilized during the Late Bronze and Early Iron Ages.*

KEY WORDS – *pottery; firing techniques; experimental archaeology; petrographic analysis; FTIR - Fourier Transform Infrared Spectroscopy analysis; Karst; Slovenia*

Raziskovanje tehnik žganja keramike v zahodni Sloveniji v pozni bronasti in starejši železni dobi na podlagi FTIR in petrografskih analiz

IZVLEČEK – *Študija je usmerjena v analizo tehnik žganja keramike v pozni bronasti in starejši železni dobi na Krasu v Sloveniji. Zaradi odsotnosti arheološki struktur smo uporabili alternativni raziskovalni pristop, in sicer FTIR in keramične petrografske analize. Arheološki material smo analizirali s pomočjo modela, ki smo ga razvili pri arheološkem raziskovalnem delu, žganju v jami in žganju v peči. S pomočjo raziskave smo uspešno prepoznali različne tehnike žganja, ki so bile v uporabi v pozni bronasti in starejši železni dobi.*

KLJUČNE BESEDE – *keramika; tehnike žganja keramike; eksperimentalna arheologija; petrografska analiza; FTIR - infrardeča spektroskopija s Fourierovo transformacijo; Kras; Slovenija*

Introduction

Archaeological research has yielded compelling evidence for pottery firing techniques during the Late Bronze and Early Iron Ages in western Slovenia. These resulted from Fourier Transform Infrared Reflectance Spectroscopy (FTIR) analysis conducted on ceramic samples obtained through archaeological experiments and archaeological excavations. As there are no archaeological structures such as pottery kilns in the area that could contribute to the understanding of firing techniques during this period, an alternative approach to the investigation is required. This paper presents the results of an investigation that sought to identify indirect evidence for Late Bronze and Early Iron Age firing practices in western Slovenia.

 DOI: 10.4312/dp.51.19

The existing knowledge of pottery technology and production during this period in the study area derives from limited research, primarily from a macroscopic point of view and focusing solely on settlement material, such as storage, cooking, and serving types of vessels. The pottery is locally produced and handmade, fired in bonfires/pit-fires and single-chamber kilns. Typological analysis indicates a clear influence from the west, particularly from the Veneto and Friuli regions in northern Italy.

The application of the Fourier Transform Infrared Reflectance Spectroscopy (FTIR) has been proven as an excellent method for identifying the mineralogical composition of archaeological ceramics and estimating firing temperatures (*Shoval, Paz 2015; Shoval 2016*). Such information can contribute significantly to the reconstruction of firing structures and to a more nuanced comprehension of firing techniques. This research comprises an interdisciplinary study of ceramics from two hillforts: (a) the Tabor site, spanning the Late Bronze to Early Iron Age, situated near Vrabče, and (b) the Štanjel site, representative of the Early Iron Age site (Fig. 1).

In addition to the aforementioned FTIR analyses, ceramic petrographic thin-section analyses were conducted on ceramic materials procured from both sites, focusing on forms presumed to be of local production. The validation of local pottery production serves to draw conclusions about the firing structures in the examined area.

Furthermore, an archaeological experiment-based model was built to facilitate the comparison with the archaeological material. This involved the recreation of probable firing techniques and conditions from the Late Bronze and Early Iron Ages, accomplished through the construction of a one-chamber kiln and the replication of vessels using local clays.

Archaeological background

The prehistoric Karst Plateau

The Karst Plateau is a landscape between the Gulf of Trieste and the Vipava Valley. In the northwest, it is connected with the Soča Plain, in the southwest with the Brkini Hills, the Podgorje Karst Plateau with the Čičarija Plateau, and the Podgraje Lowland (*Perko, Kladnik 1998*). The Karst Plateau is famous for the so-called hillforts (sl. *gradišča*, it. *castellieri*), which are dated to the Bronze and/or Early Iron Ages (*Marchesetti 1903*). Most of these hillforts were poorly excavated and the stratigraphy was preserved only in a few cases (*Canarella 1975–1977; Moretti 1978; Novaković, Turk 1991; Bratina 2014; 2021; Zupančič, Vinazza 2015; Maggi* et al. *2017; Borgna* et al. *2018; Bernardini* et al. *2023*).

The archaeological material under consideration was collected from two hillforts, Tabor near Vrabče and Štanjel. The chronological framework for both sites was established through stratigraphic analysis, and confirmed by both archaeological evidence and absolute data (*Vinazza 2021.Fig. 5*). The Tabor near Vrabče site with a double dry-wall has two occupational phases. The initial phase is dated to the end of the Late Bronze Age (10th century BC), while the second corresponds to the Early Iron Age (8th and 7th centuries BC). In contrast, the Štanjel site contains the foundations of a cellar dug into the limestone bedrock, dating to the conclusion of the end of the Early Iron Age (6th and 5th centuries BC) (*Vinazza 2021.429,442, Fig. 5*).

Pottery firing in the Late Bronze and Early Iron Ages in Slovenia

The first archaeometric study about Bronze and Iron Age firing techniques on Slovenian pottery was conducted in 2021 (*Vinazza, Dolenec 2021*). Existing research in Slovenia has been limited to individual archaeological sites, as evidenced by studies such as Janez Dular (*1982*), Matija Črešnar (*2006*), Andreja Žibrat Gašparič *et al.* (*2018*), with macroscopic analysis of ceramic technology still dominating the literature. Since we are dealing with both direct and indirect data pertaining to pottery firing at this time in Slovenia, a comprehensive understanding is possible through an overview of the current state of research.

Macroscopic and microscopic examinations of pottery technologies, constituting indirect data, suggest the utilization of both bonfires/pit fires and kilns. Notable examples include the Poštela and Novine sites in northeastern Slovenia, as well Štanjel, Tabor near Vrabče, and Tomaj in the Karst region (*Žibrat, Dolenec 2015; Žibrat* et al. *2018.188; Vinazza, Dolenec 2021.401; Vinazza 2022*).

Meanwhile, only a limited number of archaeologically excavated kilns, serving as direct data, have been identified for pottery production. Regardless of the type, these kilns are predominantly of the one-chamber type, as documented by Irena Horvat Šavel (*1988–1989. 130–131*) and Draško Josipović *et al.* (*2016*). Although the two-chamber kiln, excavated archaeologically, is dated to the Late Iron Age (*Tomanič Jevremov, Guštin 1996*), evidence from neighbouring northern Italian sites suggests its use in the Late Bronze Age (*Levi 2010. 117*), but most examples of such kilns are known from the Early Iron Age (*Poggiani Keller 1994.76; Iaia, Moroni Lanfredini 2009.65,68,70; Gasparini, Miari 2017.24; Rapi* et al. *2019.107*).

The absence of archaeologically excavated kilns is notable at the Late Bronze and Early Iron Age sites in the Karst, yet indirect data allude to their probable existence (see *Vinazza 2021; Vinazza, Dolenec 2022*). Moreover, an analysis of the *chaíne opératoire* of certain locally produced vessel types, exemplified by the ceramic situlae from the Štanjel site, suggests the use of two-chamber kilns. This specific pottery requires an oxidation-reduction-oxidation (ORO) firing atmosphere, achievable only in such kilns. By analysing the provenance based on petrographic thin-section analysis we can distinguish between local and non-local production and foresee the use of this kind of firing technique in the area under study. This research aims to compare the firing model derived from archaeological experiments using FTIR analyses, which is based on temperature estimation. Additionally, the study seeks to ascertain whether the results of FTIR analyses of

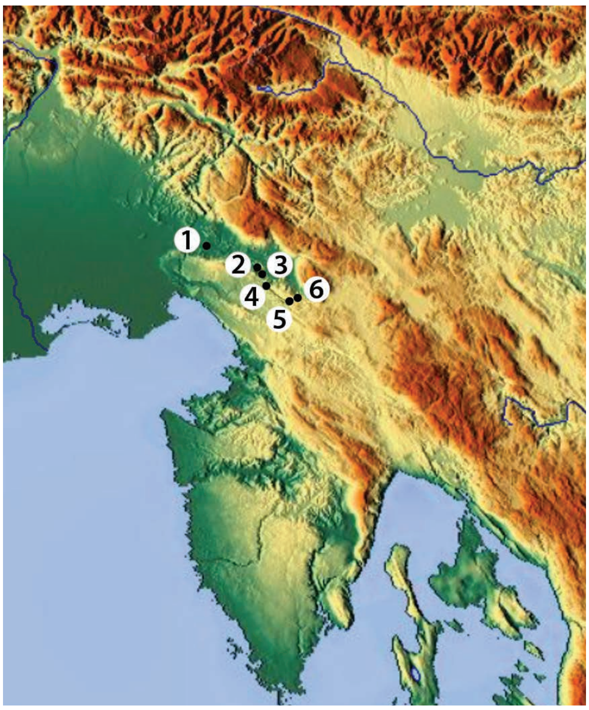

Fig. 1. A map showing the location of the clay sources (1 Renče, 2 Ostri vrh, 4 Veliki Dul, 5 Griže) and the archaeological sites (3 Štanjel, 6 Tabor near Vrabče). Source: https://maps-for-free.com/

archaeological material can effectively differentiate between pottery fired in a bonfire/pit fire and that fired in a kiln.

Geological background of the Karst Plateau

The Karst Plateau is a flat plain with conical hills, small elevations, denuded karst areas, sinkholes, caves and the average altitude above sea level is 300 to 600 metres above sea level. Despite the absence of surface streams, the plateau harbours a significant underground stream system, one that gathers available water and directs it towards the spring of Timav (*Jurkovšek* et al. *1996.21*).

Tabor near Vrabče

The archaeological site of Tabor near Vrabče (Fig. 2) encompasses two main lithostratigraphic units: the Lipica Formation and the Flysch. The Lipica Formation locally contains the Tomaj limestone, a platy and laminated limestone with chert. The limestone is bedded and massive with rudist biostromes and bioherms (*Jurkovšek* et al. *1996.25, App*.). Cherts occur in the Tomaj limestone as nodules and thin lenses and have a microcrystalline texture (*Jurkovšek* et al. *1996.47*). The Flysch unit results from the alteration of marl, sandy siltstone and coarse-grained carbonate sandstone, with intercalations of breccia and conglomerate, which consist mainly of fragments and pebbles of older carbonate platform formation. The breccia and conglomerate varieties encompass basalt conglomerate and calcite-cemented breccia, featuring limestone fragments of diverse sizes (*Jurkovšek* et al. *1996.63*).

Štanjel

The archaeological site of Štanjel lies in an even more dynamic area (Fig. 2), between four lithostratigraphic units: the Lipica Formation, the Flysch, the Liburnian Formation, the Lower Trstelj, and the Upper Trstelj beds. The Liburnian Formation comprises marly limestone and limestone breccia, while the Upper Trstelj beds, which primarily consist of miliolid limestone, exhibit calcarenite with foraminifers and Coral-algal limestone (*Jurkovšek 2010.27,40*).

Clays

Fieldwork in the wider area of interest identified various clay sources potentially suitable for pottery production. The selection of clays focused on proximity to archaeological sites (*i.e*. Tabor near Vrabče and Štanjel) and suitability for pottery production. Therefore, samples were collected from the Renče source in the

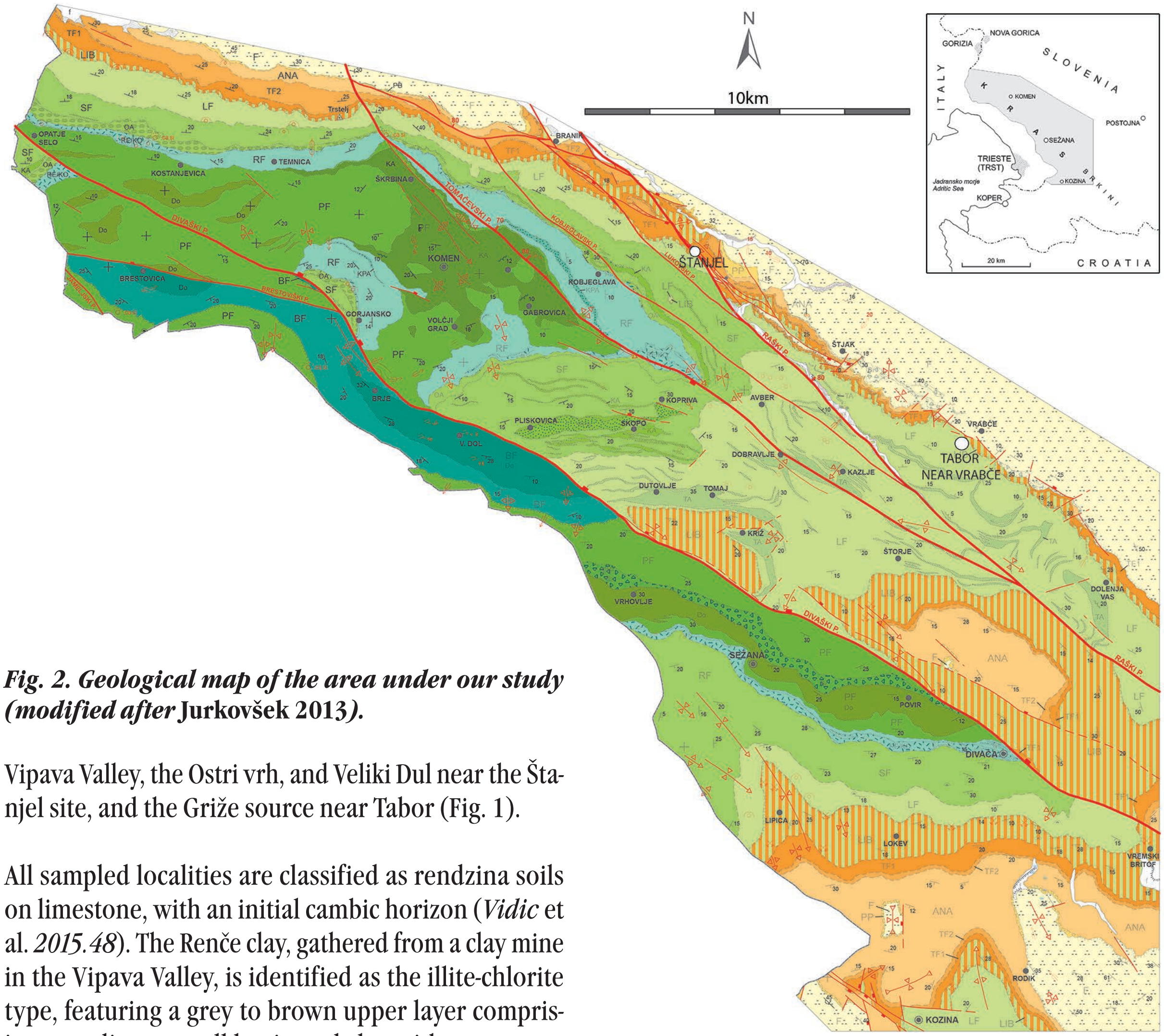

Fig. 2. Geological map of the area under our study (modified after* Jurkovšek 2013*).

Vipava Valley, the Ostri vrh, and Veliki Dul near the Štanjel site, and the Griže source near Tabor (Fig. 1).

All sampled localities are classified as rendzina soils on limestone, with an initial cambic horizon (*Vidic* et al. *2015.48*). The Renče clay, gathered from a clay mine in the Vipava Valley, is identified as the illite-chlorite type, featuring a grey to brown upper layer comprising a medium to well-laminated clay with an average thickness of 5m. The mineral composition encompasses chlorite, quartz, albite, montmorillonite, carbonate, and iron minerals (*Rokavec 2014.32,35,54*). Clays from Ostri vrh and Griže were collected on the hillsides, while the samples from Veliki Dul were collected in a valley (Fig. 1).

They fall under the terra rossa type (*Šušteršič* et al. *2009.Tab. 1*).

Materials and methods

Archaeological experiments, as detailed in Manca Vinazza (*2021a; 2021b.183–184*) and Vinazza and Matej Dolenec (*2022.392*), were conducted in the courtyard of the Department of Archaeology at the University of Ljubljana in the years 2020 and 2021. The initial phase involved the construction of a one-chamber kiln, utilizing Renče clay. Subsequently, ceramic vessels were made from the examined clay sources, which were fired in a replicated one-chamber kiln, in a pit fire and an electric laboratory kiln.

Archaeological pottery was sampled from two sites, Tabor near Vrabče and Štanjel, from which we obtained stratified material with absolute ^{14}C dates. We selected material that we were confident was locally produced, including storage and cooking vessels, as well as a locally made ceramic situla fired in ORO conditions. We sampled local clay sources in the vicinity of both archaeological sites: Griže near Tabor, and Veliki Dul and Ostri vrh near Štanjel.

Furthermore, the experimental pottery served for comparisons with archaeological pottery. To achieve this, samples from both the experimental and archaeological pottery were taken and analysed through FTIR spectroscopy (*Parish* et al. *2013*) and petrographic study of ceramic thin sections (*Quinn 2022*). Additionally, the findings from these techniques were complemented by previously acquired X-ray Diffraction (XRD) results (see Tab. 1).

FTIR Spectroscopy

The FTIR equipment employed for this research was located in the Charles McBurney Laboratory for Geoarchaeology, based in the Department of Archaeology at the University of Cambridge. Representative FTIR spectra were obtained from all the clay and ceramic samples (n=21) by grinding a few tens of micrograms of the sample using an agate mortar and pestle (*Smith 2011*). About 0.1mg or less of the sample was mixed with about 80mg of KBr (IR-grade). A 7mm pellet was then made using a hand press and the spectra were collected between 4000 and 400cm^{-1} at 4cm^{-1} resolution, using a Thermo Nicolet 380 spectrometer. The interpretation of the spectra was conducted by combining the internal library of infrared spectra of archaeological materials (Kimmel Standards) and the appropriate reference (*Weiner 2010; Chukanov 2014; Shoval, Paz 2015; Shoval 2016*).

Ceramics are produced by firing clay raw materials, which during this process undergo a series of reactions and transform into the final product. Using the FITR technique the main components of this final product can be identified (*Weiner 2010; Chukanov 2014*). This allows us to determine what was the original composition of the raw material and estimate the firing temperatures of this process (*Shoval, Paz 2015; Shoval 2016*). The most common components reported in archaeological pottery/ceramics are clay minerals (*e.g.*, kaolinite, smectite), quartz and calcite, and they are recognized on the FTIR spectra by specific bands (Tab. 1).

The raw clay component transforms through firing to fired-clay, also defined as meta-clay (*Shoval* et al. *2011a; 2011b*). The transformation occurs over a process called dehydroxylation during which the raw clay loses the water (H_2O) from its structure. Depending on the type of clay, this process takes place at different temperatures and subsequently forms different meta-clay components (*Shoval* et al. *2011a; 2011b; Shoval, Paz 2015*). A clay material dominated by kaolinite transforms into meta-kaolinite and the dehydroxylation occurs at 450–500°C (*Frost, Vassallo 1996*). A clay material dominated by smectite transforms into meta-smectite and this transformation occurs at *c.* 600°C (*Heller-Kallai, Rozenson 1980*).

Meanwhile, calcite decomposes through a thermal process called decarbonation (*Shoval 2016*). During this process carbon dioxide (CO_2) is released from the mineral's structure and free-lime (CaO) is formed (*Fabbri* et al. *2014*). The decarbonation of calcite in ceramics takes place under prolonged firing at temperatures between 600 and 800°C (*Maggetti* et al. *2011*). After long-lasting high firing temperatures (800°C and above), part of the free-lime is re-carbonated and crystallized as reformed calcite (*Shoval* et al. *2011b; Fabbri* et al. *2014*). The presence of a calcareous (calcite-rich) component in the raw material is very important since it greatly affects the thermal reactions and the firing process (*Fabbri* et al. *2014; Shoval 2016*).

Petro thin-section analysis

Petrographic analysis took place at the Laboratory for Material Analysis Laboratory within the Department of Archaeology at the University of Ljubljana. The preparation of ceramic thin sections adhered to a standard protocol (see *Quinn 2022.23–36*), and the examination was conducted under the polarizing Zeiss Axio Scope A1 microscope. Three distinct groups of ceramic material were chosen. The first is associated with the Renče clay source (Samples 1, 2, 5 and 7). The second group is linked with the Tabor near Vrabče site (Samples 11 and 18), while the third pertains to the Štanjel site (Samples 9 and 13).

Archaeological experiments

The experimental kiln was made of Renče clay that was tempered with straw. After the completion of the experiment, samples were collected from the base (Sample 2), the chimney (Sample 3), and the wall (Sample 4), which was taken 10cm above second thermocouple. During the experiment two thermocouples were placed at the base of the kiln, one under the fired vessels and the other adjacent to the wall (see *Vinazza, Dolenec 2021.Fig. 3*). The temperature measured with the thermocouples in the experimental kiln was 670°C. Several pots were fired in the experimental kiln, including Sample 1, modelled from Renče clay; Sample 10 modelled from Veliki Dul clay; and Sample 11 modelled from Griže clay. All of these pots were tempered with calcite.

In accordance with recent research by Richard Thèr *et al*. (*2018*), which proposed a model for distinguishing firing structures based on soaking time duration, we conducted experiments firing two clay cubes (5x5x 5cm) from Renče clay in a laboratory kiln. The first cube (Samples 5 and 6) was fired at 600°C, while the second cube (Samples 7 and 8) was fired at 800°C.

Tab. 1. Samples 1–21 which are part of our study.

Sam-ple	Lab ID	ITEM	Description	Firing structure	Clay	Tem-per	Firing structure	Maxi-mum	Other
1	2022-2	Vessel	Rim of the bowl	Archaeological experiment	Renče	Calcite	Replica of the kiln	670 °C	XRD (*Vinazza, Dolenec 2022.Sample 2*)
2	2022-3	Kiln	Bottom of the kiln	Archaeological experiment	Renče	Straw	Replica of the kiln	670 °C	XRD (*Vinazza, Dolenec 2022.Sample 3*)
3		Kiln	Chimney of the kiln	Archaeological experiment	Renče	Straw	Replica of the kiln	670 °C	XRD (*Vinazza, Dolenec 2022.Sample 5*)
4	2021-4	Kiln	Wall of the kiln	Archaeological experiment	Renče	Straw	Replica of the kiln	670 °C	XRD (*Vinazza, Dolenec 2022.Sample 4*)
5	2022-23	Cube	Core	Laboratory firing	Renče	0	Electrically operated kiln	600 °C	XRD (*Vinazza, Dolenec 2022.Sample 6*)
6	2022-23	Cube	Outer surface	Laboratory firing	Renče	0	Electrically operated kiln	600 °C	XRD (*Vinazza, Dolenec 2022.Sample 6*)
7	2022-24	Cube	Core	Laboratory firing	Renče	0	Electrically operated kiln	800 °C	XRD (*Vinazza, Dolenec 2022.Sample 7*)
8	2022-24	Cube	Outer surface	Laboratory firing	Renče	0	Electrically operated kiln	800 °C	XRD (*Vinazza, Dolenec 2022.Sample 7*)
9	2022-4	Silo	Štanjel site, US 28	Archaeological pottery					
10	2020-18	Vessel	Part of the vessel	Archaeological experiment	Veliki Dul	Calcite	Replica of the kiln	670 °C	
11	2020-24	Vessel	Part of the vessel	Archaeological experiment	Griže	Calcite	Replica of the kiln	670 °C	
12		Vessel	Part of the vessel	Archaeological experiment	Renče	Calcite	Pit fire	702 °C	
13	2022-1	Situla	Štanjel site, US 28	Archaeological pottery					
14		Clay		No manipulation	Renče				
15		Clay		No manipulation	Veliki Dul				
16		Clay		No manipulation	Griže				
17		Clay		No manipulation	Ostri Vrh				
18	2020-4	Pithos	Tabor near Vrabče site, US 18, outer surface	Archaeological pottery					
19	2020-4	Pithos	Tabor near Vrabče site, US 18, core	Archaeological pottery					
20	M349	Pot	Štanjel site, US 42, core	archaeological pottery					
21	M349	Pot	Štanjel site, US 42, outer surface	Archaeological pottery					

The last experimental sample (Sample 12) was pit fired in 2021, as documented by Vinazza (*2021.61, Fig. 1*). The firing reached temperatures of 702°C in less than one hour, with a subsequent cooling time lasting two hours and 41 minutes.

Archaeological material

Archaeological material comes from two sites. Beginning from the Tabor near Vrabče site, archaeological research (*Vinazza 2021.Pl.1:1*) established that the pithos (Sample 18, 19) belonged to the first occupation phase (Late Bronze Age). Macroscopic technological analysis data indicated the prevalence of a reduction atmosphere (*O.c.432*), yet it remains unclear whether the firing technique involved a bonfire/pit fire or a kiln.

From the Early Iron Age, we sampled material from the Štanjel site. A silo (Sample 9), was chosen first due to its status as the most diverse material within the site's assemblages and its local origin. It is presumed that the firing was not conducted in a kiln type (or related) structure. Based on its diameter of up to 100cm and a wall thickness of 5cm, it was believed to have been fired at low temperatures (*Vinazza 2016.9,11*) in a bonfire.

The next archaeological find from the Štanjel site is a ceramic situla (Sample 13), which, based on macroscopic analysis, is believed to have been fired in a double-chamber kiln, as this type of pottery vessel requires an ORO firing (*cf. Aloupi-Siotis 2020.3,5*).

The last vessel from the Štanjel site is a pot (*Vinazza 2021.Pl.6: 8*) from which samples were taken from the core and outer surface (Samples 20, 21).

Results

FTIR Spectroscopy

The analysed material has been categorized into three main groups. Initially, we examined the raw materials, encompassing analysis of four different clay sources. Subsequently, the experimental material was investigated, comprising materials collected from both the kiln and pottery. Finally, attention was directed towards the archaeological material.

Raw material

Renče clay (App. 5: 14)

The spectrum from the Renče clay source recorded a principal Si-O stretching band at $1028cm^{-1}$ which is indicative of smectite (Kimmel Standards). The dominance of this mineral is further supported by the shoulder band at $913cm^{-1}$ and the band at $3620cm^{-1}$. The Si-O/Al-O bending mode at $469cm^{-1}$ can equally relate to smectite and quartz (*Weiner 2010*; Kimmel Standards), although research on clay and pottery has assigned this mode based on the overlap between these two minerals reported in such materials (*Shoval 2016*). The presence of quartz is confirmed by the characteristic band-doublet at 778 and $798cm^{-1}$, and the minor peak at $695cm^{-1}$. The spectrum also recorded a shoulder band at $1166cm^{-1}$, which is related to SiO_2 mineral polymorphs (*e.g.*, tridymite, cristobalite, quartz) (*Chukanov 2014*). Clay materials contain small amounts of water in their mineralogical structure and/or between the layers of these minerals (*Wenk, Bulakh 2016; Kumari, Mohan 2021*). The presence of such water is detected by the very broad H_2O-stretching band at $3422cm^{-1}$ and the H_2O bending mode at $1637cm^{-1}$.

The band at $528cm^{-1}$ is assigned to kaolinite–montmorillonite based on previous work on this type of clay minerals (*Chukanov 2014*). Montmorillonite, in general, is the most prominent member of the smectitic group of clay minerals (*Kumari, Mohan 2021*), and very often interstratifies with other clay minerals (*e.g.*, kaolinite, illite), which further supports its existence in this sample. The band at $528cm^{-1}$ could also be related to albite (plagioclase – Na-feldspar) and muscovite (mica mineral), which are minerals commonly found within clay materials (*Chukanov 2014; Kumari, Mohan 2021*). However, the spectrum did not record any of the indicative bands of these minerals, so the likelihood of their presence is low.

Veliki Dul clay (App. 5: 15)

The spectrum from the Veliki Dul clay source recorded a principal Si-O stretching band at $1032cm^{-1}$, which is associated with smectite. The dominance of this mineral is supported by the shoulder band at $913cm^{-1}$, the bands at $3620cm^{-1}$ and $534cm^{-1}$, and the minor peak at $3692cm^{-1}$. The combined Si-O/Al-O bending mode at $469cm^{-1}$ is again considered the result of the overlap between smectite and quartz (*Shoval 2016*). The presence of quartz is confirmed by the characteristic band-doublet at 777 and $797cm^{-1}$, and the minor peak at $694cm^{-1}$. Water, related to the clay components, is recorded by the very broad H_2O-stretching band at $3438cm^{-1}$ and the H_2O bending mode at $1637cm^{-1}$. The band at $534cm^{-1}$ could again relate to muscovite or albite, but for the same reasons as with the Renče sample it is attributed to the kaolinite–montmorillonite.

Griže clay (App. 6: 16)
The spectrum from the Griže clay source is very similar to those collected from the samples of Renče clay and Veliki Dul clay sources. It is dominated by smectite based on the principal Si-O stretching band (1032cm^{-1}) and the bands at 3693cm^{-1}, 3620cm^{-1}, 915cm^{-1}, and 531cm^{-1}. The combined Si-O/Al-O bending mode at 469cm^{-1} is regarded as the result of the overlap between smectite and quartz. Clay-related water is recorded by the very broad H_2O-stretching band at 3422cm^{-1} and the H_2O bending mode at 1637cm^{-1}. Furthermore, quartz is identified by the characteristic band-doublet at 777 and 797cm^{-1} and the minor peak at 695cm^{-1}. The spectrum also included a shoulder band at 1165cm^{-1} that is related to SiO_2 mineral polymorphs.

Ostri vrh clay (App. 6: 17)
The spectrum from the Ostri vrh clay source has many similarities with the ones collected from the other three sources. The principal Si-O stretching band at 1031cm^{-1} the shoulder band at 913cm^{-1}, the bands at 3620cm^{-1} and 531cm^{-1}, and the minor peak at 3691 cm^{-1} indicate the dominance of smectite in this sample. Meanwhile, the combined Si-O/Al-O bending mode at 470cm^{-1} is again considered the result of the overlap between smectite and quartz. Clay-related water is again recorded by the H_2O-stretching band at 3422 cm^{-1} and the H_2O bending mode at 1637cm^{-1}. Lastly, the presence of quartz is confirmed by the characteristic band-doublet at 779 and 798cm^{-1} and the minor peak at 694cm^{-1}.

Experimental material (2020)
Base (App. 1: 2)
The spectrum of the sample collected from the base of the Kiln recorded a principal Si-O stretching band at 1036cm^{-1} which is associated with a meta-clay (*i.e.* fired-clay). Considering that this band falls within the range of 1030–1060cm^{-1}, the main component of this sample is meta-smectite (*Shoval 2016*). Besides the main band, the spectrum includes a shoulder band at 1090cm^{-1}, suggesting that this sample also includes meta-kaolinite. The dominance of meta-clay in this sample is further supported by the combined Si-O/Al-O bending mode at 469cm^{-1}, which is also related to the fired-clay material (*O.c.*).

Clay-related water is also detected by the very broad H_2O-stretching band at 3422cm^{-1} and the H_2O bending mode at 1636cm^{-1} (*Shoval 2016*). The meta-clay ceramics, being dehydrated after firing, strongly absolve water (*i.e.* absorbed water) during a slow rehydration process (*Muller* et al. *2000*; *Shoval, Paz 2013*). Quartz is identified by the characteristic band-doublet at 779 and 798cm^{-1}, the minor peak at 695cm^{-1} and the shoulder band at 520cm^{-1}. Lastly, the shoulder band at 1166cm^{-1} and the weak band at 1870cm^{-1} are associated with SiO_2 mineral polymorphs.

The presence of the meta-smectite suggests that this ceramic material endured temperatures around 600°C (*Heller-Kallai, Rozenson 1980*). However, the spectrum recorded a minor band at 3621cm^{-1}, which is attributed to raw smectite (*i.e.* retains its original structure). This suggests that the firing procedure did not consistently maintain high temperatures (600°C and above) and allowed the preservation of a small raw smectitic component. Meanwhile, the presence of meta-kaolinite does not support temperatures below 450°C, so the base probably experienced temperatures between 450 and 650°C.

Wall (App. 2: 4)
The spectrum of the wall sample recorded a principal Si-O stretching band at 1040cm^{-1} which is indicative of meta-smectite since it falls within the range of 1030–1060cm^{-1}. Moreover, it presented a shoulder peak at 1085cm^{-1} that is assigned to the overlap occurring between quartz and meta-kaolinite. The combined Si-O/Al-O bending mode at 469cm^{-1} further confirms that meta-clay is the principal component of this sample.

Absorbed water, associated with the meta-clay unit, is detected by the H_2O-stretching band at 3421cm^{-1}. Quartz is identified by the characteristic band-doublet at 779 and 798cm^{-1}, and the minor peak at 694cm^{-1}. The spectrum also included a minor band at 1618cm^{-1} that is related to SiO_2 mineral polymorphs. In comparison to the base's sample, this one has a calcareous component. A main CO_3 band at 1437cm^{-1} and a secondary band at 879cm^{-1} have been recorded, which are characteristic of calcite. Moreover, the spectrum recorded a minor band at 729cm^{-1}, which is indicative of dolomite.

The presence of meta-smectite and the absence of raw smectite suggest that this ceramic material endured high firing temperatures (>600°C). The main CO_3 band falls within the range of 1430–1450cm^{-1}, which is associated with reformed calcite (*Shoval 2016*). The presence of this type of calcite suggests firing temperatures consistently above 700°C. Meanwhile, the spectrum did not present bands assigned to 'firing silicates' (*i.e.* around 912cm^{-1}), which would indicate temperatures above 800°C (*Shoval 2016*). These findings indicate that these walls were exposed to temperatures between 700 and 800°C that led to the complete transformation of the main components of the clay material (*i.e.* clay and calcite).

Chimney (App. 1: 3)
The spectrum of the chimney sample recorded a principal Si-O stretching curve that splits into two peaks. The first at 1082cm^{-1} is generally associated with quartz (*Saikia* et al. *2008*) but in pottery samples it is regarded as the result of the overlap between quartz and meta-kaolinite (*Shoval, Paz 2015*). Meanwhile, the second peak at 1038cm^{-1} is indicative of meta-smectite. The combined Si-O/Al-O bending mode found at 465cm^{-1} supports that meta-clay and quartz are the main components of this sample.

The considerable presence of quartz, in addition to the Si-O stretching band, is confirmed by the characteristic band-doublet at 778 and 797cm^{-1}, and the minor peak at 694cm^{-1}. Moreover, the minor band at 1618cm^{-1} and the shoulder band at 1164cm^{-1} are both associated with SiO_2 mineral polymorphs. Absorbed water, associated with the meta-clay unit, is detected with the H_2O-stretching band at 3421cm^{-1} and the H_2O bending mode at 1637cm^{-1}.

Regarding the firing temperature, the presence of meta-smectite and the absence of bands attributed to raw smectite suggest that this sample experienced high firing temperatures (>600°C). Meta-kaolinite retains its structure for temperatures up to 950°C (*Shoval 2016*; *Stevenson, Gurnick 2016*), while the meta-smectite starts to show signs of distortion at temperatures above 900°C (*Stevenson, Gurnick 2016; Tarhan, Işık 2020*). Such signs are not recorded in the spectrum, suggesting that this sample was exposed to temperatures between 600 and 900°C for a sufficient amount of time.

Pot 1 (App. 1: 1) (Renče clay)
A pot was made from Renče clay that was tempered with calcite and fired within the experimental kiln. The FTIR analyses recorded a principal Si-O stretching band at 1082cm^{-1}, which is considered the result of the overlap between the quartz and the meta-kaolinite component (*Shoval, Paz 2015*). The combined Si-O/Al-O bending mode at 462cm^{-1} is also attributed to the overlap between these two components. The important presence of quartz is further identified by the characteristic band-doublet at 778 and 797cm^{-1}, and the minor peak at 694cm^{-1}. The spectrum also recorded a minor band at 1618cm^{-1} and a shoulder band at 1166cm^{-1} that are both associated with SiO_2 mineral polymorphs (*Chukanov 2014*). Absorbed water, associated with the meta-clay is detected with the H_2O bending mode at 1638cm^{-1}. In contrast, the spectrum did not detect a calcite component in the examined sample. Meta-kaolinite is formed at 450 to 500°C (*Frost, Vassallo 1996*) and retains its structure up to 950°C (*Shoval 2016; Stevenson, Gurnick 2016*). Since no other recorded component can provide further information on the firing temperatures, it is considered that this experimental pot was fired at temperatures between 450 and 900°C.

Pot 2 (App. 4: 12), Renče clay
Another pot was made from Renče clay that was also tempered with calcite but fired in a pit fire. The collected spectrum recorded a principal Si-O stretching band at 1036cm^{-1}, which is indicative of a meta-smectite. There is also a shoulder peak at 1085cm^{-1} which is attributed to the overlap between the quartz and the meta-kaolinite component. The dominance of the meta-clay in the sample is supported by the combined Si-O/Al-O bending mode at 473cm^{-1}. Meanwhile, raw smectite is reported by the minor band at 3620cm^{-1} and a band at 521cm^{-1}. Water associated with the clay components (*i.e.* raw and meta) is detected by the broad H_2O-stretching band at 3422cm^{-1} and the H_2O bending mode at 1637cm^{-1}.

Quartz is identified by the characteristic band-doublet at 779 and 797cm^{-1}, and the minor peak at 695cm^{-1}. The spectrum also recorded a minor band at 1872cm^{-1} and a shoulder band at 1164 that are related to SiO_2 mineral polymorphs. Furthermore, the spectrum has a main CO_3 band at 1420cm^{-1}, a secondary band at 875 cm^{-1},and minor bands at 1796 and 712cm^{-1}, which are characteristic of primary calcite (*Shoval 2016*).

The reported meta-clays in this sample support firing temperatures between 600°C and 900°C (*Shoval 2016; Stevenson, Gurnick 2016; Tarhan, Işık 2020*). However, the occurrence of primary calcite does not justify temperatures that go much higher than 700°C. Moreover, the detected raw clay suggests that the firing procedure did not consistently maintain high temperatures (>600°C). Based on these results, the highest temperatures reached in the pit fire was probably around 700°C, while the average firing temperatures should have been around 600°C.

Ceramic cube (App. 2: 5, 6)
A pottery cube was made from Renče clay, without tempering, and fired in the experimental kiln. The core and outer surface of this cube were sampled and analysed by FTIR. The spectra recorded a principal Si-O stretching band at 1032cm^{-1}, which is assigned to meta-smectite. They also present a combined Si-O/Al-O bending mode (at 469cm^{-1} for the core and 472cm^{-1} for the outer surface, respectively) that relates to the meta-clay component and subsequently supports that this cube mostly consisted of meta-smectite. Meanwhile, the neighbouring shoulder peaks (at 1090cm^{-1} and 1085cm^{-1} respectively) are attributed to the overlap between quartz and a meta-kaolinite component. Nevertheless, the pottery cube retains parts of the raw clay that was not affected by the firing. The FTIR analyses recorded a broad band at 3620cm^{-1}, a shoulder band at 913cm^{-1} and a band at 532cm^{-1} (core) and 525cm^{-1} (outer surface) that are characteristic of raw smectite. These bands, in particular, are associated with kaolinite–montmorillonite (*Chukanov 2014*), which is a mineral also detected in the original clay material (*i.e.* Renče clay source). Furthermore, Kaolinite-montmorillonite complies with the recognized meta-clays (*i.e.* meta-smectite and meta-kaolinite) since they are the expected outcome after firing this type of mineral.

Water related to clay components is detected by the very broad H_2O-stretching band at 3421cm^{-1} and the H_2O bending mode at 1637cm^{-1} (outer surface). The presence of quartz is confirmed by the characteristic band-doublet at 779 and 797cm^{-1}, and the minor peak at 694cm^{-1}. Additionally, the spectra included minor bands at 1870 and 1618cm^{-1}, and a shoulder band at 1166cm^{-1} (1164cm^{-1} for the outer surface) that are related to SiO_2 mineral polymorphs.

The presence of the meta-smectite suggests that this ceramic material was exposed to temperatures around 600°C and above (*Heller-Kallai, Rozenson 1980*). The examined sample, though, retains a raw clay component (*i.e.* kaolinite–montmorillonite) suggesting that the firing did not consistently maintain high temperatures (>600°C). Meanwhile, the presence of meta-kaolinite does not support temperatures below 450°C, so this pottery cube was probably fired at temperatures between 450 and 650°C.

Ceramic cube 2 (App. 3: 7, 8)
Another pottery cube was made from Renče clay, without tempering, but fired in an electric kiln. Similar to the previous cube, samples were collected from the core and outer surface, and analysed by FTIR. The core's spectrum recorded a principal Si-O stretching band at 1082cm^{-1} which is the result of the overlap between the quartz and a meta- kaolinite. The Si-O asymmetrical bending vibration at 457cm^{-1} is more compatible with quartz rather than a meta-clay. The increased presence of this mineral is further confirmed by the characteristic band-doublet at 778 and 797cm^{-1}, and the minor peak at 694cm^{-1}. The spectrum also recorded minor bands at 1870 and 1618cm^{-1}, and shoulder bands at 1164 and 557cm^{-1} that are related to SiO_2 mineral polymorphs. These findings suggest that SiO_2 mineral polymorphs (*e.g.*, quartz) are the dominant component of this cube's core. Lastly, absorbed water related to the meta-clay component is detected by the H_2O-stretching band at 3421cm^{-1}.

The outer surface's spectrum recorded a principal Si-O stretching curve that splits into two peaks. The first is at 1036cm^{-1} and it is assigned to meta-smectite, while the second peak at 1086cm^{-1} is the result of the overlap between the quartz and the meta-kaolinite component of the sample. The dominance of the meta-clay in this sample is further supported by the combined Si-O/Al-O bending mode at 470cm^{-1}. Absorbed water is detected by the very broad H_2O-stretching band at 3421cm^{-1} and the minor H_2O bending mode at 1637 cm^{-1}. Regardless, this sample also holds a strong content of SiO_2 mineral polymorphs. Quartz is identified by the characteristic band-doublet at 779 and 797cm^{-1}, and the minor peak at 694cm^{-1}, where other SiO_2 polymorphs are detected by the two shoulder bands at 1164cm^{-1} and 561cm^{-1}.

Regarding the firing temperature, the presence of only meta-kaolinite in the core of this pottery cube suggests that it was broadly exposed to temperatures between 450°C and 900°C (*Frost, Vassallo 1996; Shoval 2016*; *Stevenson, Gurnick 2016*). In contrast, the sample of the outer surface also contains meta-smectite, which along with the absence of raw clay indicates that this part of the cube was exposed at higher firing temperatures (>600°C) and more precisely between 600°C and 900°C (*Shoval 2016; Stevenson, Gurnick 2016; Tarhan, Işık 2020*).

Pot 3 (App. 4: 11), Griže clay
This pottery sample was made of Griže clay that was tempered with calcite and fired within the experimental kiln. The FTIR analyses recorded a principal Si-O stretching curve that splits into two peaks. The first

at $1082cm^{-1}$ is assigned to the overlap between the quartz and the meta-kaolinite. Meanwhile, the second at $1046cm^{-1}$ falls within the range of $1030–1060cm^{-1}$ relating to a meta-smectite composition. The dominance of the meta-clay in the sample is supported by the combined Si-O/Al-O bending mode at $473cm^{-1}$.

Absorbed water is detected by the very broad H_2O-stretching band at $3421cm^{-1}$. Quartz is identified by the characteristic band-doublet at 777 and $797cm^{-1}$, and the minor peak at $694cm^{-1}$. The spectrum also included two minor bands at 1872 and $1618cm^{-1}$ and a shoulder band at $1164cm^{-1}$ that are related to SiO_2 mineral polymorphs. Lastly, the small CO_3 band at $1420cm^{-1}$ is associated with primary calcite (*Shoval 2016*).

The reported meta-clays in the sample support firing temperatures between 600°C and 900°C (*Shoval 2016; Stevenson, Gurnick 2016; Tarhan, Işık 2020*). However, the occurrence of primary calcite does not justify temperatures much higher than 700°C. Therefore, this pottery sample was fired at temperatures between 600 and 700°C.

Pot 4 (App. 4: 10), Veliki Dul clay
This pottery sample was made of Veliki Dul clay, which was tempered with calcite and fired within the experimental kiln. The collected spectrum recorded a principal Si-O stretching curve that splits into two peaks. The first peak at $1039cm^{-1}$ is related to meta-smectite, while the second peak at $1086cm^{-1}$ is again associated with the overlap between the quartz and the meta-kaolinite. The dominance of the meta-clay component is further supported by the combined Si-O/Al-O bending mode at $473cm^{-1}$. Absorbed water related to the meta-clay is detected by the broad H_2O-stretching band at $3420cm^{-1}$.

Quartz is identified by the characteristic band-doublet at 777 and $797cm^{-1}$, and the minor peak at $694cm^{-1}$. The spectrum also recorded minor bands at 1870 and $1617cm^{-1}$ and a shoulder band at $1166cm^{-1}$ that are related to SiO_2 mineral polymorphs. Meanwhile, the main CO_3 band at $1421cm^{-1}$ and the bands at 1793, 878 and $713cm^{-1}$ are assigned to calcite, and based on the value of the main CO_3 band it is described as primary calcite (*Shoval 2016*). Lastly, the spectrum included a band at $3480cm^{-1}$ that it has not been possible to relate to any suitable mineral/component.

Regarding the firing conditions, the meta-clay supports fire temperatures between 600°C and 900°C. However, the occurrence of primary calcite does not justify temperatures much higher than 700°C. Therefore, this pottery sample was most probably fired at temperatures between 600 and 700°C.

Pithos (App. 6–7: 18, 19), Tabor near Vrabče
Samples from the core and outer surface of a pithos (from the Tabor near Vrabče site) were collected and analysed by FTIR. The core's spectrum recorded a principal Si-O stretching band at $1032cm^{-1}$ which is indicative of a meta-smectite. The combined Si-O/Al-O bending mode at $473cm^{-1}$ is also attributed to the meta-clay. However, the band at $534cm^{-1}$ is characteristic of kaolinite–montmorillonite and shows that the sample retains a small part of the original raw clay. Water, associated with the clay components (*i.e.* raw and meta), is detected by the H_2O-stretching band at $3448cm^{-1}$ and the H_2O bending mode at $1637cm^{-1}$. Meanwhile, the main CO_3 band at $1429cm^{-1}$, the secondary band at $875cm^{-1}$, and the minor bands at 2512, 1797 and $712cm^{-1}$, are indicative of calcite. Based on the value of the main CO_3 band, this is further described as primary calcite (*Shoval 2016*). Moreover, quartz is identified by the characteristic band-doublet at 779 and $799cm^{-1}$.

The outer surface's spectrum recorded a principal Si-O stretching band at $1028cm^{-1}$ which is associated with raw smectite. Moreover, the band at $534cm^{-1}$ is attributed to kaolinite–montmorillonite (*Chukanov 2014*) and further supports the dominance of raw clay in this sample. The Si-O/Al-O bending mode at $473cm^{-1}$, however, is related to a meta-clay component, which in this case is a meta-smectite. Water, related to the clay components (*i.e.* raw and meta), is detected by the H_2O-stretching band at $3422cm^{-1}$ and the H_2O bending mode at $1637cm^{-1}$. Equally with the core, the outer surface also contains an important quantity of calcite. This is recorded with a main CO_3 band at $1425cm^{-1}$, a secondary band at $875cm^{-1}$, and minor bands at 2512, 1794 and $712cm^{-1}$. Based on the value of the main CO_3 band this is also described as primary calcite (*Shoval 2016*). Moreover, quartz is identified by the characteristic band-doublet at 779 and $797cm^{-1}$.

Regarding the firing conditions, the presence of meta-smectite and primary calcite supports temperatures between 600 to 800°C. However, the detected raw clay (*i.e.* kaolinite–montmorillonite) indicates that the firing also included temperatures below 600°C. It seems that the core of the pithos was fired for a longer period and at high temperatures than the outer surface. We discuss about this in the discussion part and it is not neccesary an error.

Silos (App. 3: 9), Štanjel
This sample was taken from a large silo that was made from a large clay band. The spectrum recorded a principal Si-O stretching band at 1032cm^{-1} which is indicative of a meta-smectite. The combined Si-O/Al-O bending mode at 476cm^{-1} is also related to the meta-clay and confirms that this is the main component of this sample. Absorbed water is detected by the very broad H_2O-stretching band at 3431cm^{-1} and the H_2O bending mode at 1636cm^{-1}. Quartz is identified by the characteristic band-doublet at 778 and 797cm^{-1}, and the minor peak at 694cm^{-1}. The spectrum also included a shoulder band at 1165cm^{-1} that is related to SiO_2 mineral polymorphs. Moreover, the spectrum also reported a main CO_3 band at 1420cm^{-1}, a secondary band at 874cm^{-1}, and a minor band at 712cm^{-1}, which are characteristic of calcite.

The main CO_3 band is assigned to primary calcite (*Shoval 2016*), suggesting firing temperatures below 800°C. Meanwhile, the presence of meta-smectite and the absence of raw clay indicate that this pottery was consistently fired at 600°C and above. Hence this silo was exposed to firing temperatures between 600 and 700°C.

Ceramic situla (App. 5: 13)
The spectrum of this sample recorded a principal Si-O stretching band at 1036cm^{-1} which is indicative of a meta-smectite. Moreover, there is a shoulder peak at 1085cm^{-1} that is assigned to the overlap between quartz and meta-kaolinite. The combined Si-O/Al-O bending mode at 474cm^{-1} is also related to the meta-clay and confirms that it is an important component of this sample. The spectrum reported the significant presence of calcite, which was identified by a main CO_3 band at 1420cm^{-1}, a secondary band at 875cm^{-1}, and minor bands at 2513, 1794 and 712cm^{-1}. Furthermore, absorbed water is detected by the H_2O-stretching band at 3421cm^{-1} and the H_2O bending mode at 1637cm^{-1}. Quartz is identified by the characteristic band-doublet at 779 and 798cm^{-1}. The spectrum also included a band at 1618cm^{-1} that is related to SiO_2 mineral polymorphs.

The presence of meta-smectite and the absence of a raw clay component suggest that this ceramic find was fired at high temperatures (>600°C), which resulted in the complete transformation of the original clay. Meanwhile, the main CO_3 band is associated with primary calcite (*Shoval 2016*), suggesting firing temperatures below 800°C. The ceramic situla was thus exposed to firing temperatures between 600 and 700°C.

Pot (App. 7: 20, 21)
Samples from the core and outer surface of a pottery fragment were collected and analysed by FTIR. The spectra recorded a principal Si-O stretching band at 1028cm^{-1} which is associated with raw smectite. Moreover, the band at 534cm^{-1} (at 535cm^{-1} for the outer surface) is attributed to kaolinite–montmorillonite (*Chukanov 2014*) and further supports the dominance of raw clay in this pottery fragment. The Si-O/Al-O bending mode at 474cm^{-1}, however, is related to a meta-clay component which in this case is a meta-smectite. Water, related to the clay components (*i.e.* raw and meta), is detected by the H_2O-stretching band at 3422 cm^{-1} (at 3423cm^{-1} for the outer surface) and the H_2O bending mode at 1637cm^{-1}. Quartz is identified by the characteristic band-doublet at 778 and 798cm^{-1} (at 779 and 798cm^{-1} for the outer surface). Additionally, the spectrum recorded the important presence of calcite with a main CO_3 band at 1425cm^{-1}, a secondary band at 875cm^{-1}, and minor bands at 2512, 1794 and 712cm^{-1}.

Having raw smectite as the principal component generally indicates low firing temperatures (<600°C). However, the presence of a small meta-smectite particle suggests that for a short period the fire reached temperatures of 600°C and above. The main CO_3 band falls within the range of 1420–1430cm^{-1} and is associated with primary calcite (*Shoval 2016*), suggesting firing temperatures below 800°C. Therefore, this pottery fragment was most likely exposed to firing temperatures around 600°C.

Ceramic petro thin-section
The initial focus in the ceramic petro thin-sections involved the analysis of Renče clay, revealing two distinct different fabric types. Sample 2 (Fig. 3.1), derived from a kiln base, exhibits a fabric consistent with firing structures observed in archaeological sources (*e.g.*, *Quinn 2022.Figs.3.53, 7.12*). The presence of numerous irregularly oriented planar voids due to the burning out of organic matter – in this case straw – is a characteristic feature. The preparation of the clay was less precise compared to that seen with the vessels, resulting in poorly sorted and individually closed inclusions. Inclusions, comprising quartz, muscovite mica,

clay pellets, calcite, and ferruginous minerals, occur naturally in the clay and constitute 40% of the composition. Organic matter was used as a temper. Sample 1 (pot 1, tempered with calcite; Fig. 3.2) has the same clay matrix as Sample 2 but lacks organic matter and calcite temper. Similarly, there are no differences in the clay matrix among the remaining two samples made from the Renče clay (Samples 5 and 7) (Tab. 1).

The subsequent group pertains to the Tabor near Vrabče site and consists of two samples: one experimentally made from Griže clay (Sample 11; Fig. 3.3), tempered with calcite, and another from a pithos fragment (Sample 18; Fig. 3.4). The inclusions recorded in these samples, encompassing mono- and polycrystalline quartz, iron opaque minerals, muscovite mica, and iron-rich clay pellets, constitute 30% of the sample. The majority of these inclusions appear as equant rounded or elongate rounded particles, with quartz reported as equant subangular. They exhibit a single-spaced and randomly aligned distribution, occasionally forming locally oriented planes, resulting in a coarse fabric. Meanwhile, in the pithos (Samples 18, 19) we identified the presence of calcite and grog temper. The calcite grains exhibit intentional cracking, showing equant angular to equant subangular shapes. Additionally, rare grog was detected, a characteristic feature of this period (see *Vinazza 2021.433*). Other inclusions include mono- and polycrystalline quartz, muscovite mica, iron-rich clay pellets, and iron-opaque minerals. The clay matrix reveals evidence of intentional clay mixing, contributing to its moderate heterogeneity. Approximately 10% of the sample is occupied by macro and micro-sized voids, characterized as planar and channel-shaped. These voids are attributed partly to firing cracks and partly to the remnants of burned organic matter, utilized as temper, albeit in minimal quanti-ties.

The third group pertains to the Štanjel site and constitutes the most diverse group, involving the analysis of local clay from Veliki Dul (Sample 10; Fig. 3.5), a presumably local pottery type known as a silo (Sample 9; Fig. 3.6), a local pot (Sample 20; Fig. 3.7), and a presumably imported ceramic situla (Sample 13; Fig. 3.8). The Veliki Dul clay has 40% inclusions, among which calcite, mono- and polycrystalline quartz, muscovite mica, iron-rich clay pellets and opaque iron minerals were identified. The silo, presumably tempered with calcite, grog, and partially burned organic matter, features macro- and mega-sized channel-shaped voids (Fig. 3). Quartz is the predominant inclusion, but muscovite mica, iron-rich clay lumps, iron-rich opaque minerals, flint, zircon, and feldspar (indicative of igneous rocks) were also present. Arranged individually, these contribute to a coarse fabric which constitutes 40% of the overall composition. Similarly, the fragment of the local pot (Sample 20) encompasses 55% inclusions, with calcite dominating at 90%. Apart from a minimal presence of grog grains (0,1%), calcite prevails as the temper. Other identified inclusions include monocrystalline quartz, muscovite mica, and iron-rich clay pellets. The homogeneous clay matrix represents 40% of the sample, accompanied by 5% of micro-sized vughs voids irregularly orientated within the clay matrix.

The ceramic situla (Sample 13) was tempered with calcite speleothem grains, originating from stalagmite/stalactite formations, along with grog and clay lumps. The clay lumps exhibit visible cracks, potentially linked to the incorporation of fine clay material that underwent drying before being mixed with the clay. Other inclusions encompass mono- and polycrystalline quartz, limestone, flint, iron-rich clay pellets, iron-opaque minerals, and muscovite mica. Notably, muscovite mica is more prevalent in the grog than in the clay matrix. Planar macroscopic voids are evident, associated with the drying process and the forming of the vessel, particularly those that are parallel in orientation.

The petrographic results within the Renče group align with the referencing model for various ceramic forms, including vessels and structures. A comparative analysis between the pottery from Tabor near Vrabče (Sample 18) and the local clay (Sample 11) validates its local provenance. Moreover, the pottery was tempered with calcite, grog, and organic matter, consistent with the prevalent practices during the Late Bronze and the beginning of the Early Iron Age. The Štanjel group yields even more interesting results. While Pot 5 is identified through a comparison with experimental material sourced from local Veliki Dul clay, the same cannot be asserted for the silo, which incorporates components of igneous rock not native to the Karst. Conversely, the ceramic situla exhibits a composition entirely derived from local material.

Discussion

Petrographic analysis has elucidated the utilization of both local and non-local clay sources in archaeological ceramics. Given the geological diversity of Slovenia, which influences the composition of clay sources, we employed a singular clay source, such as Renče clay,

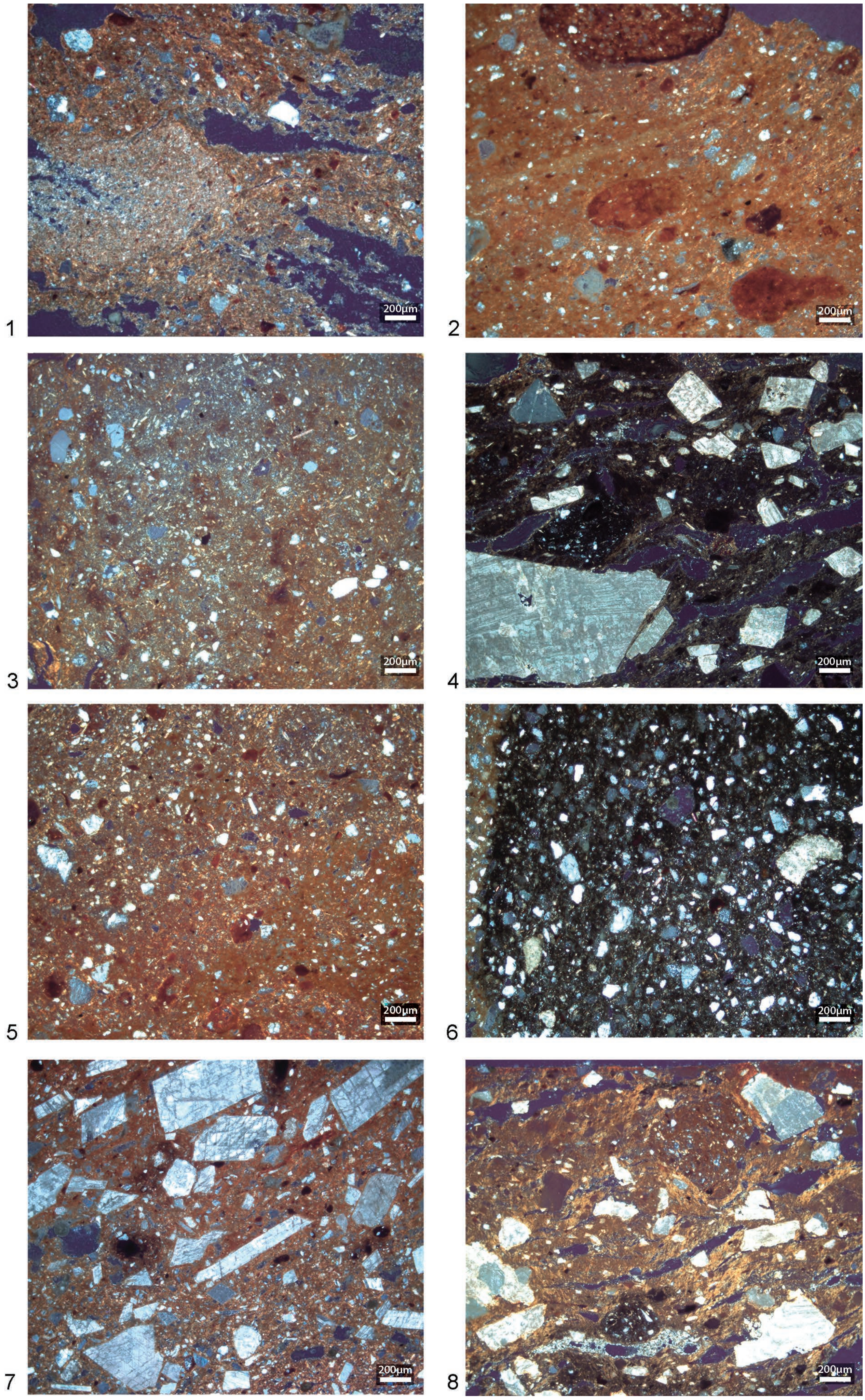

Fig. 3. Ceramic thin-section. Photos taken under plain polarized light.

throughout the entire operational sequence – from pot shaping to pot firing. Additionally, for processes occurring in different firing structures we utilized other clay sources from the vicinity of the aforementioned archaeological sites (Fig 1).

The samples from all four clay sources predominantly exhibit a smectitic clay composition. Moreover, those from the Renče and Veliki Dul clay sources indicated the presence of kaolinite-montmorillonite, a clay mineral polymorph that combines kaolinitic and smectitic compositions. Quartz is consistently recorded as the second most abundant mineral in all the examined sources. However, the FTIR results did not detect bands assigned to calcite in any of the clay sources.

The FTIR analyses of experimental clay revealed that the kiln dominantly consists of meta-clay and exhibits a higher quartz content. Meta-clay is characterized by a combination of kaolinitic and smectitic origins, reflecting the clay minerals present in the original clay source. Unexpectedly, findings from the wall (Sample 4) indicate the presence of a small calcite component. Calcite was not reported in the original clay, and possibly these related to small pebbles that were in the outcrop that was sampled.

The FTIR results additionally indicate that the base of the kiln was exposed to lower firing temperatures compared to the wall and chimney. The presence of raw clay in the base's sample suggests temperatures ranging between 450 and 650°C, while neither the wall nor chimney retain any traces of raw material. The composition of the chimney supports a wide range of high temperatures (*i.e.* 600 and 900°C), while the presence of reformed calcite in the wall's sample is indicative of temperatures between 700 and 800°C.

The suggested temperatures align with those recorded by two thermocouples during the conducted experiment. They indicated that the temperature near the wall exceeded 600°C for at least 30 minutes, while at the base it was maintained for at least two hours. The temperature at the base gradually increased, reaching around 600°C by the end of the firing procedure. Meanwhile, the temperature rise along the wall did not exhibit a similar pattern, possibly due to the incomplete loading of the kiln and the vessels not being in direct contact with the kiln wall. The sample from the wall of the kiln was taken 10cm above second thermocouple, implying that the selected sample area was in direct contact with the fire, resulting in temperatures higher than those at the bottom base. AMS measurements (*Vinazza, Dolenec 2022.Fig. 3*) agree with the FTIR results, and the lower temperatures at the base probably relate to the fact that the sampled area was under the vessels and eventually not in direct contact with the fire. The occurrence of the different temperatures at the different parts of a kiln was confirmed by thermovision camera measurements in another archaeological experiment conducted in 2018 (*Vinazza 2021.Fig. 150*). The temperature measured with thermocouples in the experimental kiln was 670°C, closely corresponding to the samples taken from the base of the kiln *i.e.* between 450 and 650°C. Furthermore, the XRD results help refine and narrow down lower temperature estimates, confirming firing above 550°C (*Vinazza, Dolenec 2022.396*). Combining the FTIR and XRD results yields a final estimated firing temperature ranging from 550 to 650°C. This suggests that the FTIR results reflect the firing process very well and help us better understand its complexity. Additionally, the complexity of these results emphasizes the importance of thoughtful consideration before sampling archaeological material.

The FTIR results for a pot (Sample 1) initially indicated a broad temperature range between 450 and 900°C, but subsequent XRD results, as reported by Vinazza and Dolenec (*2002.396*), refined the temperature estimate to between 550 and 900°C.

The FTIR results of the firing pot in pit firing (Sample 12) displayed temperatures around 700°C, aligning closely with the firing temperatures measured by a thermocouple. Despite the short heating time, the FTIR accurately reflected the process. The FTIR results for the pottery samples modelled from local clay Veliki Dul (Sample 10) and Griže (Sample 11) indicated that both pottery vessels were composed of meta-clay, quartz, and calcite, suggesting firing temperatures between 600 and 700°C. These findings fit well with temperatures measured by thermocouples during the firing procedure (*i.e.* 670°C).

In order to distinguish firing structures based on soaking time, the FTIR analyses are also very helpful. FTIR results for the first cube indicate exposure to temperatures ranging from 450 to 650°C. The core retained some raw clay, suggesting lower temperatures (450 and 600°C), consistent with the understanding that the core requires more time to fire. Conversely, the outer surface showed no presence of the raw clay, indicating prolonged exposure to higher temperatures

(>600°C). For the second cube, the FTIR results clearly demonstrated an overall exposure to higher temperatures (>600°C). The dominance of meta-clay and quartz, coupled with the complete absence of raw clay, suggested temperatures between 600 and 900°C, aligning with the temperatures achieved in the electric kiln (*i.e.* 800°C).

Since these results confirmed the laboratory firing temperatures we can also use this method for the archaeological material.

The final step of our investigation involved the application of FTIR and petrographic analyses to archaeological materials, aiming to interpret the firing process that was employed.

Starting with the Tabor near Vrabče site, both the outer surface (Sample 18) and core (Sample 19) of the pithos were analysed. The FTIR analyses of the outer surface revealed a predominance of raw smectite, signifying low firing temperatures. Nevertheless, a small meta-smectite component was identified, indicating that for a brief period high temperatures were reached (between 600 to 800°C). In contrast, the core exhibited an increased meta-clay component, indicating consistent exposure to higher temperatures (>600°C). These odd temperature findings between the outer surface and the core may be connected to the vessel's position during firing, where heat is radiated from the interior to the vessel's exterior or temperature drop during firing, characteristics more indicative of a bonfire/pit fire rather than of a kiln.

Thin-section analysis revealed that this silo (Sample 9) was tempered with calcite, organic matter, and grog. Moreover, the clay matrix included minerals typical of igneous rocks, which are not naturally occurring in the Karst plateau. Notably, it also contains a higher concentration of muscovite mica compared to the local Veliki Dul clay (Sample 10), suggesting a distinct clay origin not indigenous to the area. The FTIR results reindicated that it primarily consists of meta-smectite, quartz and primary calcite. Furthermore, the absence of raw clay suggests firing temperatures between 600 and 700°C. Given the wall thickness, an extended firing duration is required for proper firing due to the slower heat penetration. Thin-section analysis indicated temperatures not exceeding 670°C, as calcite grains did not exhibit signs of decomposition (*Vinazza, Dolenec 2022.395*).

The next archaeological find from the Štanjel site is a ceramic situla (Sample 13), which was initially presumed to be an imported ware, but petrological characteristics revealed that it was tempered with speleothem calcite, a material commonly found in the Karst caves surrounding the archaeological site. The investigation of the situla also identified the use of grog and clay lumps for tempering. Notably, the grog exhibited a significantly higher muscovite content compared to the clay matrix, indicating a distinct clay composition. The presence of a planar voids suggests a lack of proper clay preparation. This, coupled with the speleotherm calcite grains, strongly supports the local production of this situla.

Since petrographic analysis revealed no visible degradation of the calcite and the FTIR results support these findings and indicate firing temperatures between 600 and 700°C, this suggest that the situla was indeed fired under controlled environment, such as the one within a kiln. Moreover, the macroscopic examination revealed ORO firing. All these results strongly support the idea of the existence of a double-chamber kiln in the area under study during the Early Iron Age.

Pottery findings from Štanjel contribute also to a hypothesis supporting the local production of pottery using at least a one-chamber pottery kiln. To test this hypothesis a pot (Samples 20, 21) from the Štanjel site was examined. The FTIR results indicate temperatures around 600°C, consistent in both the core and outer surface, suggesting that the firing conditions were stable, devoid of temperature fluctuations, a characteristic achievable in a kiln. Furthermore, petrographic analysis revealed that the vessel was tempered with calcite, and no grain decomposition was observed, indicative of temperatures below 650°C. The ability to control the firing temperature in a kiln likely facilitated the use of calcite temper, a practice common in this region and elsewhere.

Conclusion

Archaeological investigations have unveiled the utilization of distinct firing structures by the Late Bronze and Early Iron Age communities in the Karst Plateau. A detailed examination of a variety of firing processes was conducted through the development of an interpretative model based on experimental firings.

By synthesizing results from different analyses, it becomes feasible to understand and accurately interpret the results collected from archaeological materials. This paper presents, for the first time, an investigation that was successful in detecting and confirming the utilization of firing structures during the Late Bronze and Early Iron Ages in western Slovenia. Given the absence of archaeologically excavated firing structures in this region, this type of analysis stands as the most effective means to gain insight into firing practices during that period. The research findings indicate that bonfire/pit-fires were utilized in the Late Bronze Age, while kilns became prevalent in the Early Iron Age. Notably, the presence of locally produced ceramic situlae in the Early Iron Age (6th century BC) serves as evidence for the use of double-chamber kilns during this period, predating their archaeological attestation in the Late Iron Age.

The archaeological research illuminated the complexity of firing processes and emphasized the importance of meticulous sampling to yield meaningful results and definitively answer research questions. FTIR analyses also help to detect irregularities in the firing, but special care must be given to proper sampling. Lastly, outdoor experiments provide more realistic insights into past processes, and proved to be highly suitable for cross-referencing with archaeological material.

Acknowledgements
We would like to thank Dr Angelo De Min for his kind help with mineral identification in the context of petrographic pottery thin-sections analysis and the reviewers who made the text more fruitful. Special thanks are also due to Professor Charlie French, director of the Charles McBurney Laboratory for Geoarchaeology, University of Cambridge, for his guidance and support.
The article was written within the Archaeology Research Programme at the Scientific Institute of the Faculty of Arts of the University of Ljubljana (P6-0247).

∴

References

Aloupi-Siotis E. 2020. Ceramic technology: how to characterize black Fe-based glass-ceramic coatings. *Archaeological and Anthropological Sciences 12: 191*.
https://doi.org/10.1007/s12520-020-01136-9

Borgna E., Cássola Guida P., Mihovilić K., Tasca G., and Teržan B. 2018. Il Caput Adriae tra Bronzo Antico e Bronzo Recente. In E. Borgna, P. Cássola Guida, and S. Corazza (eds.), *Preistoria e protostoria del Caput Adriae*. Studi di preistoria e protostoria 5. Istituto italiano di preistoria e protostoria. Firenze: 75–96.

Bratina P. 2014. Tomaj. In B. Teržan, M. Črešnar (eds.), *Absolutno datiranje bronaste in železne dobe na Slovenskem/ Absolute dating of Bronze and Iron Ages in Slovenia*. Znanstvena založba Filozofske fakultete. Narodni muzej Slovenije. Ljubljana: 587–595.

2018. Bronze and Iron Age settlements in the Kras and the Vipava Valley, Slovenia. In E. Borgna, P. Cássola Guida, and S. Corazza (eds.), *Preistoria e protostoria del Caput Adriae*. Studi di preistoria e protostoria 5. Istituto italiano di preistoria e protostoria. Firenze: 173–180.

Cannarella D. 1975–1977. Il castelliere di Monrupino. *Atti della Societá per la Preistoria e Protostoria della Regione Friuli-Venezia Giulia 3: 155–161.*

Chukanov N. V. 2014. *Infrared spectra of mineralspecies; Extended library. Volume 1*. Springer Geochemistry/Mineralogy. Springer Dordrecht Heidelberg. London.

Črešnar M. 2006. Novi žarni grobovi iz Ruš in pogrebni običaji v ruški žarnogrobiščni skupini (Die neuer Urnengräber aus Ruše und das Bestattungsritual in der Ruše-Gruppe der Urnenfelderkultur). *Arheološki vestnik 57: 97–162.*
https://ojs.zrc-sazu.si/av/article/view/8272

Dular J. 1982. *Halštatska keramika v Sloveniji*. Dela SAZU. Slovenska akademija znanosti in umetnosti. Ljubljana.

Fabbri B., Gualtieri S., and Shoval S. 2014. The presence of calcite in archeological ceramics. *Journal of the European Ceramic Society 34(7): 1899–1911.*
https://doi.org/10.1016/j.jeurceramsoc.2014.01.007

Frost R. L., Vassallo A. M. 1996. The Dehydroxylation of the Kaolinite Clay Minerals using Infrared Emission Spectroscopy. *Clays and Clay Minerals 44: 635–651*.
https://doi.org/10.1346/CCMN.1996.0440506

Gasparini D., Miari M. 2017. Lo scavo del Foro Annonario di Cesena: indagini di un sito dell età del Bronzo in un contesto pluristaficato urbano. In F. Rubat Borel, M. Cupitò, C. Delpino, A. Guidi, and M. Miari (eds.), *Le età del Bronzo e del Ferro in Italia: contesti protostorici in scavi urbani. Incontri annuali di preistoria e protostoria*. II Incontro Annuale di Preistoria e Protostoria IAPP. Istituto italiano di preistoria e protostoria. Firenze: 23–26.

Grahek L., Košir A. 2018. Analiza naselbinske keramike z Mosta na Soči z vrstičnim elektronskim mikroskopom/Scanning electron microscopy analysis of the pottery from the settlement at Most na Soči. In J. Dular, S. Tecco Hvala (eds.), *Železnodobno naselje Most na Soči. Razprave/The Iron Age settlement at Most na Soči. Treatises*. Opera Instituti Archaeologici Sloveniae 34. ZRC SAZU. Ljubljana: 307–321. https://doi.org/10.3986/9789610501091

Heller-Kallai L., Rozenson I. 1980. Dehydroxylation of Dioctahedral Phyllosilicates. *Clays and Clay Minerals 28: 355–368*. https://doi.org/10.1346/CCMN.1980.0280505

Horvat Šavel I. 1988–1989. Bronastodobna naselbina Oloris pri Dolnjem Lakošu. *Arheološki vestnik 39–40: 127–145.*

Iaia C., Moroni Lanfredini A. (ed.). 2009. *L'etá del ferro a Sansepolcro. Attivita produttive e ambiente nel sto di Trebbio.* Peruggia, Aboca Edizioni.

Josipovič D., Turk M., Rupnik J., Brezigar B., Toškan B., and Kovač M. 2015. *Končno strokovno poročilo o arheološki raziskavi ob gradnji. Arheološko izkopavanje v Dobravi – Otočcu* (parc. št. 121, k. o. 1460 Šentpeter).

Jurkovšek B., Toman M., Ogolerec B., Šribar L., Šribar L., Poljan M. and Drobne K. 1996. *Formacijska geološka karta južnega dela Tržaško-komenske planote 1:50.000: kredne in paleogenske karbonatne kamnine/Geological map of the southern part of the Trieste-Komen Plateau: Cretaceous and Paleogene carbonate rocks*. Inštitut za geologijo, geotehniko in geofiziko. Ljubljana.

Jurkovšek B. 2010. *Geološka karta severnega dela Tržaško-komenske planote 1: 25 000: tolmač/Geological map of the northern part of the Trieste-Komen plateau 1: 25 000.* Geološki zavod Slovenije. Ljubljana.

2013. Geološka karta Krasa/Geological map of Kras (Slovenia). https://www.geo-zs.si/PDF/GeoloskeKarte/Kras_new.pdf

Kumari N., Mohan C. 2021. Basics of Clay Minerals and Their Characteristic Properties. In G. M. Do Nascimento (ed.), *Clay and Clay Minerals.* IntechOpen. Rijeka: 1–29. doi.org/10.5772/intechopen.97672

Levi S. T. 2010. *Dal coccio al vasaio. Manifattura, technologia e classificazione della ceramica.* Zanichelli. Bologna.

Maggetti M, Neururer C., and Ramseyer D. 2011. Temperature evolution inside a pot during experimental surface (bonfire) firing. *Applied Clay Science 53(3): 500–508.* https://doi.org/10.1016/j.clay.2010.09.013

Maggi P., Pieri F., and Ventura P. 2017. *Monte Castellier. Le pietre di Elleri narrano la storia*. Edizioni Università di Trieste. Trieste.

Marchesetti C. 1903. *I castellieri preistorici di Trieste e della regione Giulia*. Museo Civico di Storia Naturale. Trieste.

Moretti M. 1978. Complessi dai Castelliei di Nivize e Monte Grisa. In L. Ruaro Loseri (ed.), *I castellieri di Nivize, Monte Grisa, Ponte S. Quirino*. Monografia di Preistoria 1. Atti dei civici musei di storia ed arte di Trieste. Trieste: 10–26.

Muller F., Drits V., Plançon A., and Robert J. L. 2000. Structural Transformation of 2:1 Dioctahedral Layer Silicates during Dehydroxylation-Rehydroxylation Reactions. *Clays and Clay Minerals 48: 572–585*. https://doi.org/10.1346/CCMN.2000.0480510

Parish R. M., Swihart G. H., and Li Y. S. 2013. Evaluating Fourier Transform Infrared Spectroscopy as a Non-destructive Chert Sourcing Technique. *Geoarchaeology: An International Journal 28: 289–307.* https://doi.org/10.1002/gea.21437

Poggiani Keller R. 1994. L'ultima fase di vita dell'insediamento. Due fornaci per ceramica della media etŕ del ferro. In R. Poggiani Keller (ed.), *Il villaggio preistorico e le fornaci di Ponte S. Marco*. Calcinato. Ikonos: 75–89.

Quinn P. 2022. *Thin section Petrography, Geochemistry and Scanning Electron Microscopy of Archaeological Ceramics*. Archaeopress. Oxford. https://doi.org/10.32028/9781803272702

Rapi M., Quirino, T., Castellano L., Hirose M., Amato, A., Barberi E., and Busnelli S. 2019. Per scalfare, per cuocere e per produrre. Le strutture da fuoco dell' abitato etrusco del Forcello di Bagnolo S. Vito: aspetti tipologici e funzionali. In A. Peinetti, M. Cattani, and F. Debandi (eds.), *Focolari, forci e fornaci tra neolitico ed etá del ferro. Comprendere le attività domestiche e artigianali attraverso lo studio delle installazioni pirotechnologiche e dei residui di combustione.* Sesto incontro annuale di preistoria e protostoria. Università di Bologna. Bologna: 17–109.

Rokavec D. 2014. *Gline v Sloveniji*. Geološki zavod Slovenije. Ljubljana.

Saikia B. J., Parthasarathy G., and Sarmah N. C. 2008. Fourier transform infrared spectroscopic estimation of crystallinity in SiO_2 based rocks. *Bulletin of Materials Science 31: 775–779.* https://doi.org/10.1007/s12034-008-0123-0

Saracino M. 2014. *Dalla terra al fuoco. La tecnologia ceramica degli antichi Veneti*. Scienze e Lettere. Roma.

Shoval S. 2016. FTIR in Archaeological Ceramic Analysis. In A. Hunt (ed.), *The Oxford Handbook of Archaeological Ceramic Analysis*. Oxford University Press. Oxford: 509–530.

Shoval S., Paz Y. 2013. A study of the mass-gain of ancient pottery in relation to archeological ages using thermal analysis. *Applied Clay Science 82: 113–120.* https://doi.org/10.1016/j.clay.2013.06.027

2015. Analyzing the fired-clay ceramic of EBA Canaanite pottery using FTIR spectroscopy and LA-ICP-MS. *Periodico di Mineralogia 84(1): 213–231.*

Shoval S., Boudeulle M., and Panczer G. 2011a. Identification of the thermal phases in firing of kaolinite to mullite by using micro-Raman spectroscopy and curve-fitting. *Optical Materials 34.2: 404–409*.
https://doi.org/10.1016/j.optmat.2011.08.031

Shoval S., Yadin E., and Panczer G. 2011b. Analysis of thermal phases in calcareous Iron Age pottery using FTIR and Raman spectroscopy. *Journal of Thermal Analysis and Calorimetry 104: 515–525.*
https://doi.org/10.1007/s10973-011-1518-5

Smith B. C. 2011. *Fundamentals of Fourier Transform Infrared Spectroscopy*. 2nd edition. CRC Press. Boca Raton.
https://doi.org/10.1201/b10777

Stevenson C. M., Gurnick M. 2016. Structural collapse in kaolinite, montmorillonite and illite clay and its role in the ceramic rehydroxylation dating of low-fired earthenware. *Journal of Archaeological Science 69: 54–63*.
https://doi.org/10.1016/j.jas.2016.03.004

Šušteršič F., Rejšek K., Mišič M., and Eichler F. 2009. The role of loamy sediment (terra rossa) in the context of steady state karst surface lowering. *Geomorphology 106: 35–45.*
https://doi.org/10.1016/j.geomorph.2008.09.024

Tecco Hvala S. 2014. Lončene situle iz starejše železne dobe na območju Slovenije/Early Iron age ceramic situlae from Slovenia. In S. Tecco Hvala (ed.), *Studia Praehistorica in Honorem Janez Dular*. Opera Instituti Archaeologici Sloveniae 30. ZRC SAZU, Ljubljana: 323–339.
https://doi.org/10.3986/9789610503651

Thér R., Kallistová A., Svoboda Z., +3 authors, and Bajer A. 2018. How was Neolithic Pottery fired? An Exploration of the Effects of Firing Dynamics on Ceramic Products. *Journal of Archaeological Methodology and Theory 26: 1143–1175*.
https://doi.org/10.1007/s10816-018-9407-x

Tomanič Jevremov M., Guštin M. 1996. Keltska lončarska peč s Spodnje Hajdine pri Ptuju. *Arheološki vestnik 47: 267–278.*

Vidic N., Prus T., Grčman H., +8 authors, and Lobnik F. 2015. *Tla Slovenije s pedološko karto v merilu 1:250000/Soils of Slovenia with soil map 1:250000*. EUR Scientific and Technical Research Series. Luxembourgh.

Vinazza M. 2016. Silosi – posebne keramične oblike: prispevek k poznavanju gospodinjstev v starejši železni dobi na Krasu/Silos – special ceramic forms: contribution to the knowledge of the Early Iron households in the Karst region. *Arheo 33: 7–23.*

2021. Naselbinska keramika starejše železne dobe na Krasu/Settlement pottery from the Early Iron Age in Kras. *Arheološki vestnik 72: 419–452.*
https://doi.org/10.3986/AV.72.14

Vinazza M., Dolenec M. 2022. Pottery firing in the Early Iron Age in Western Slovenia. *Documenta Praehistorica 49: 388–405*. https://doi.org/10.4312/dp.49.20

Weiner S. 2010. *Microarchaeology: Beyond the Visible Archaeological Record*. Cambridge: Cambridge University Press. https://doi.org/10.1017/CBO9780511811210

Wenk H. R., Bulakh A. 2016. *Minerals, their constitution and origin*. Second edition. Cambridge University Press.

Zupančič D., Vinazza M. 2015. Suhozidna gradnja v prazgodovini na Krasu. *Kronika. Časopis za zgodovino in narodopisje 63: 691–702*.

Žibrat Gašparič A., Vinazza M., and Črešnar M. 2018. Characteristics of Early Iron Age pottery from north-eastern Slovenia through the prism of ceramic technology and petrography. *Documenta Praehistorica 45: 180–202*.
https://doi.org/10.4312/dp.45.14

Appendix 1

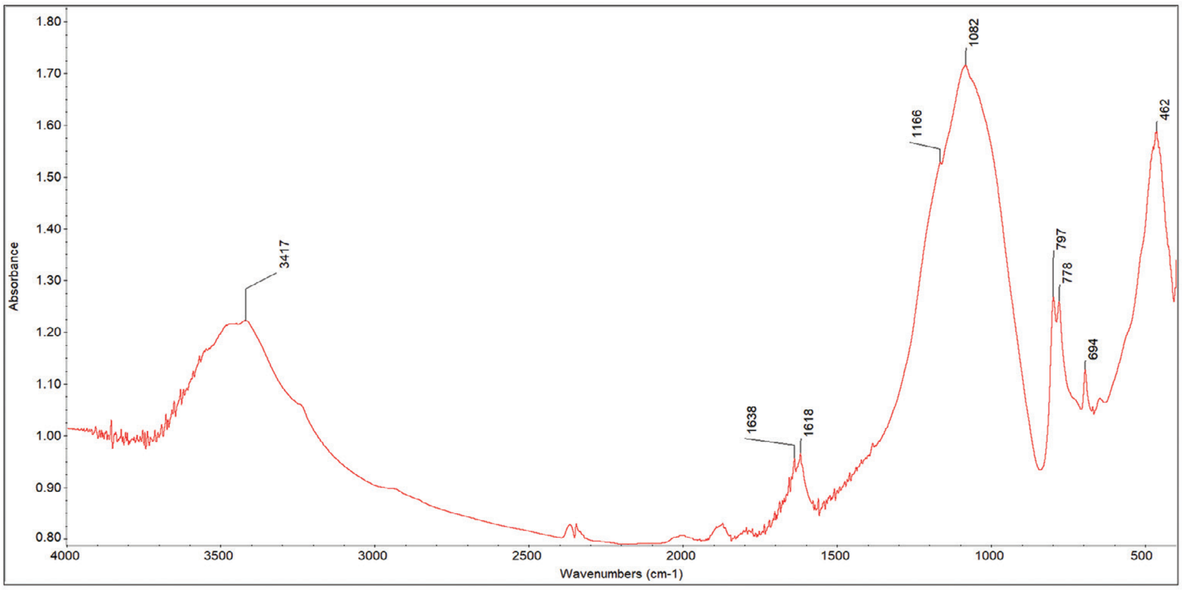

1

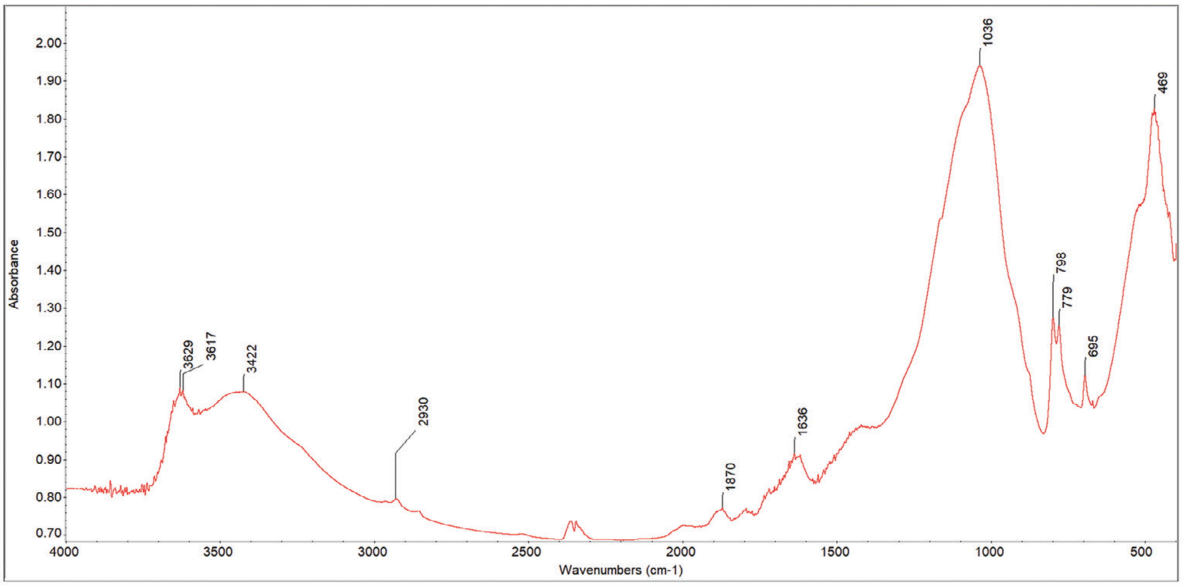

2

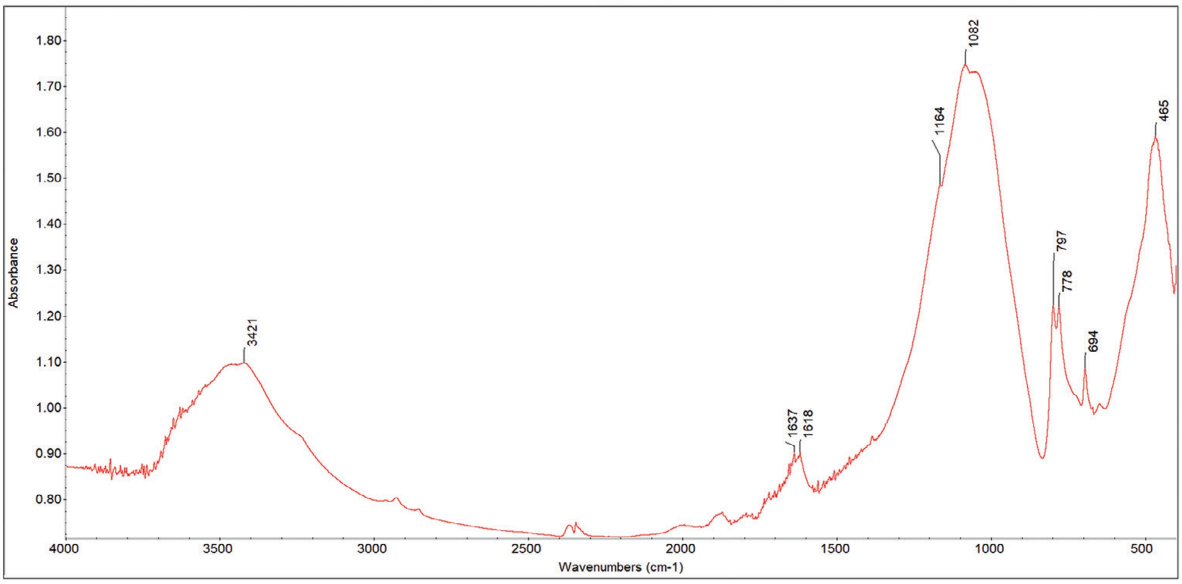

3

Appendix 2

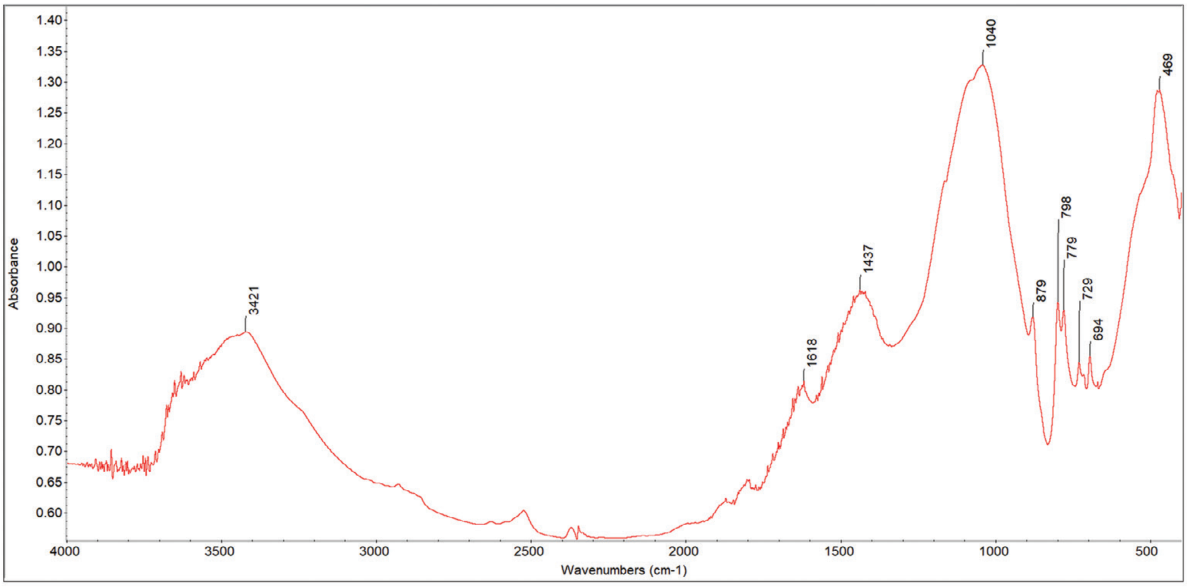

4

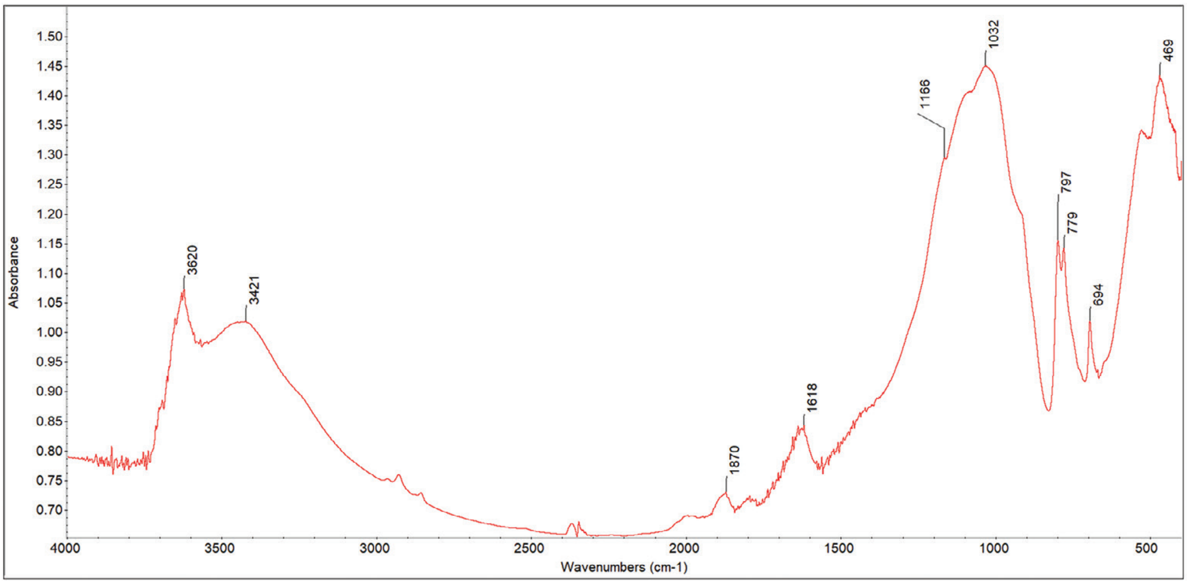

5

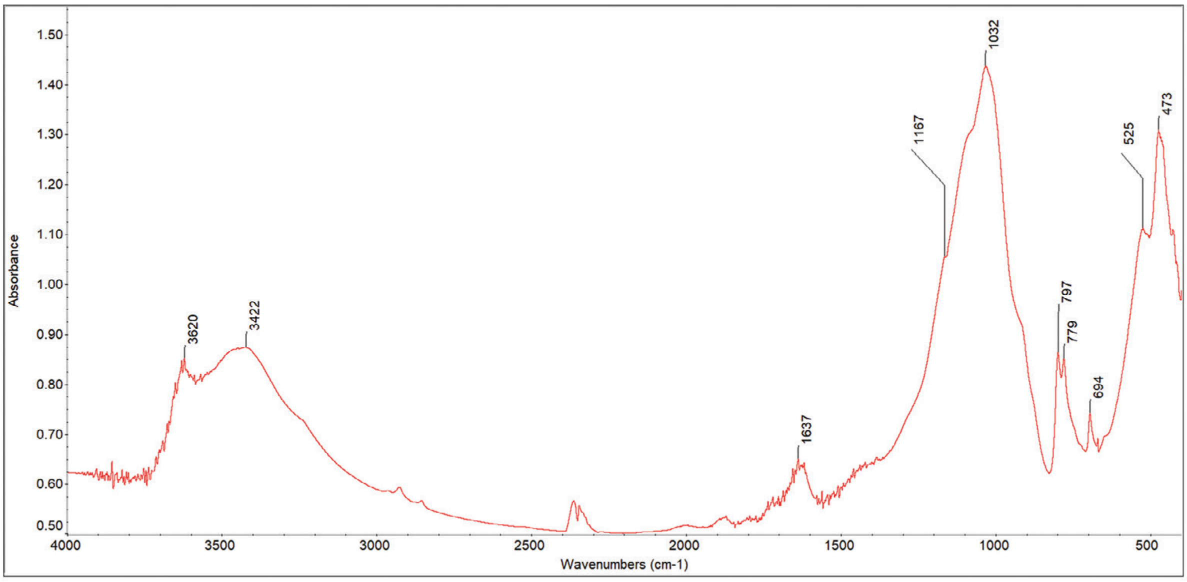

6

Appendix 3

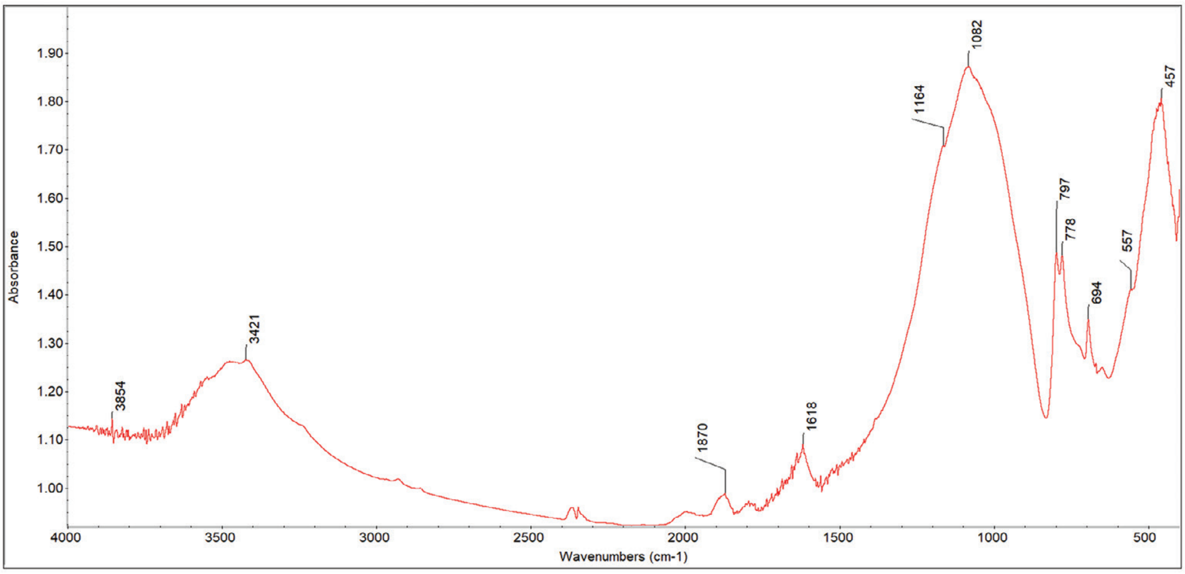

7

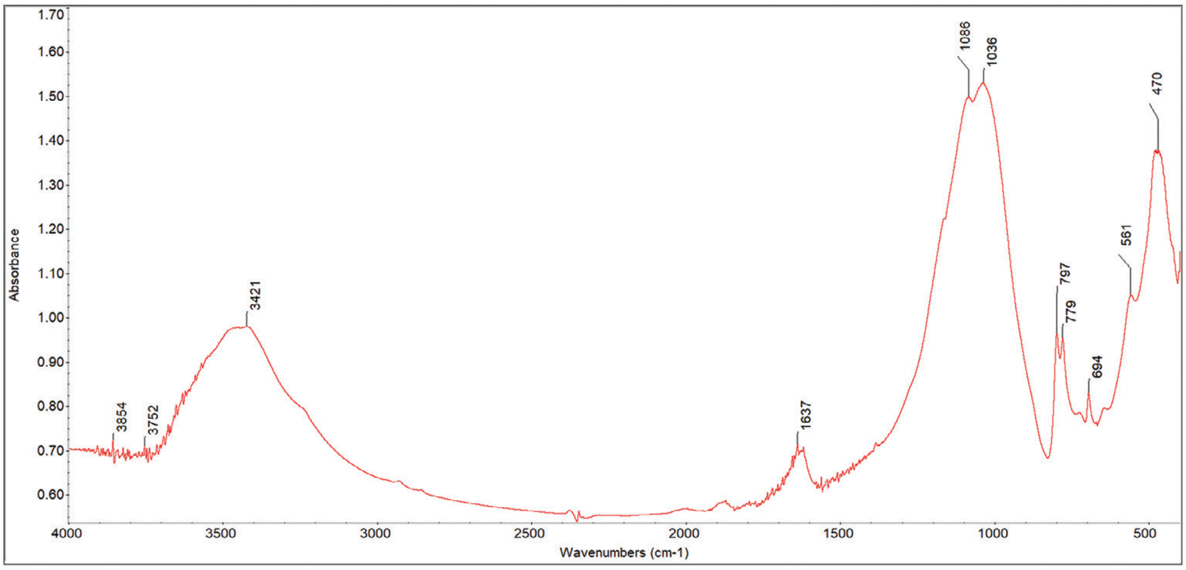

8

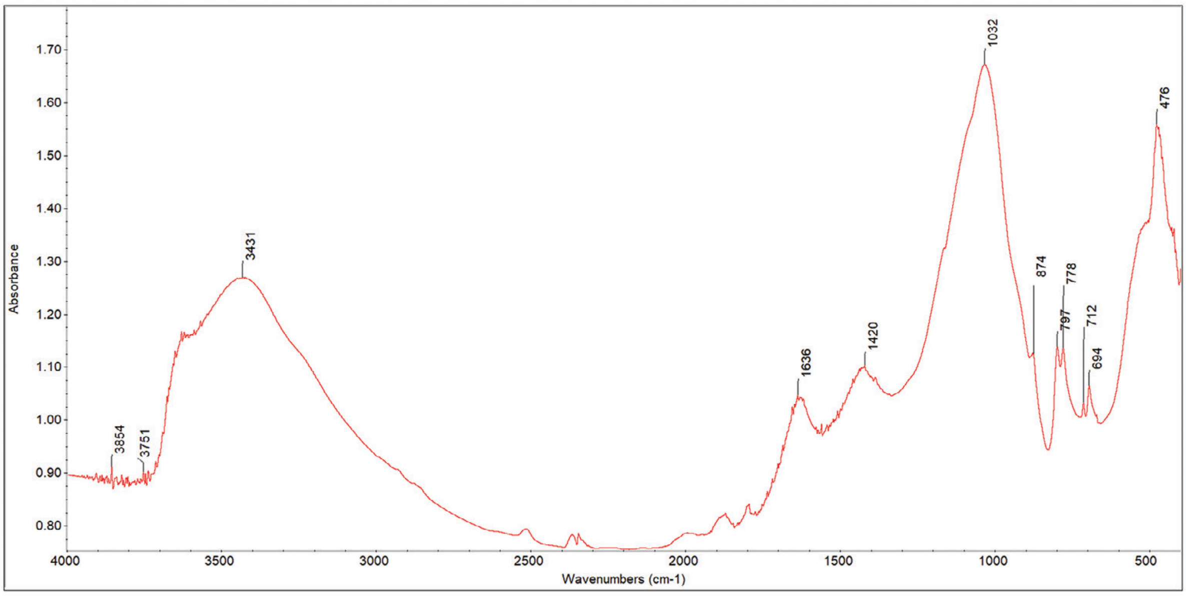

9

Appendix 4

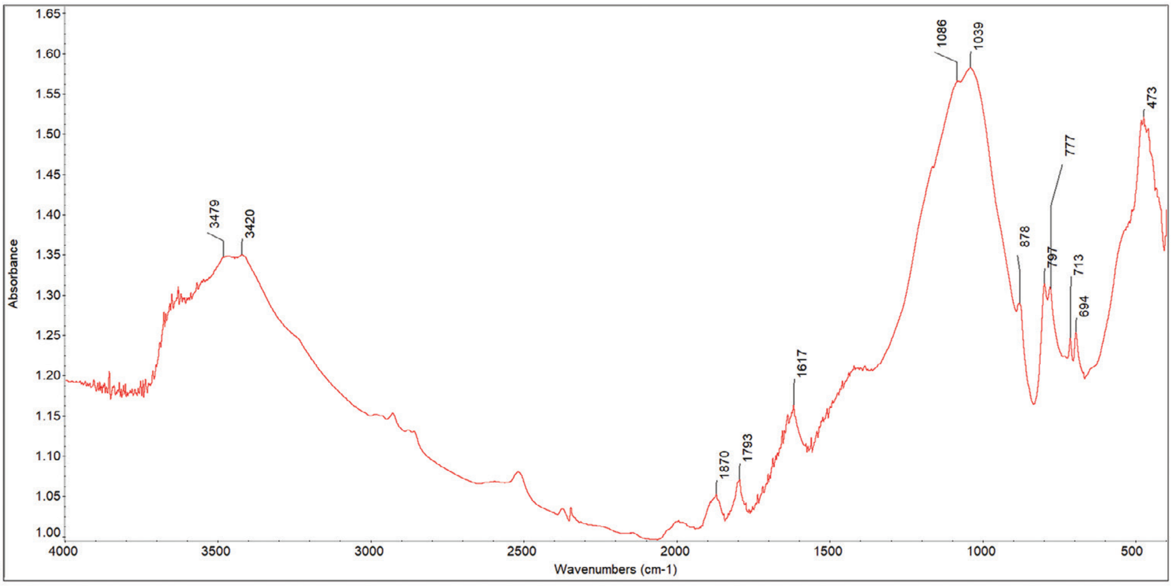

10

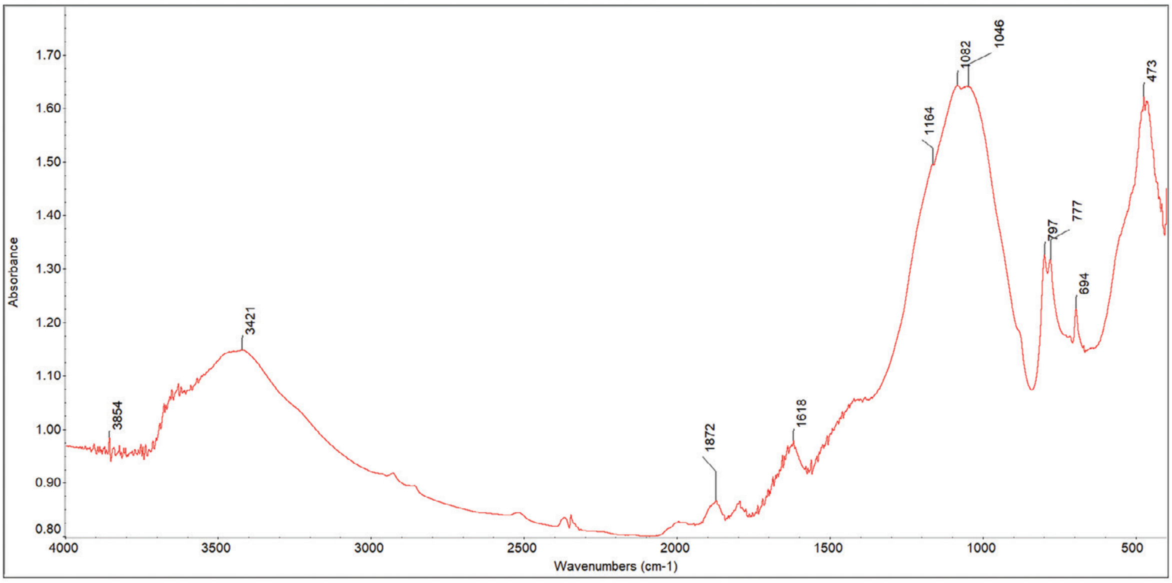

11

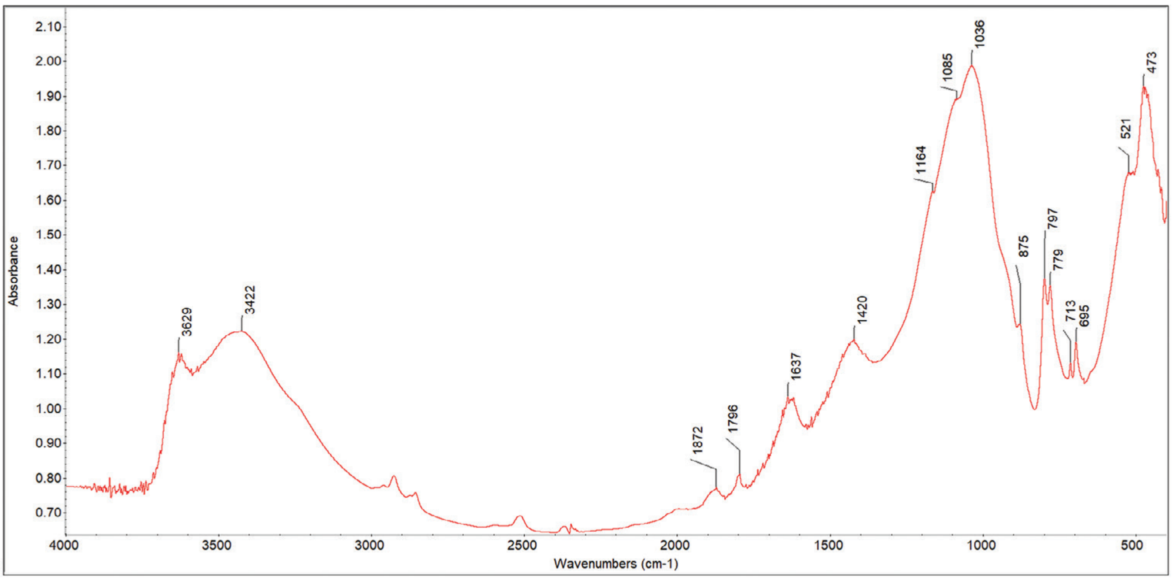

12

Appendix 5

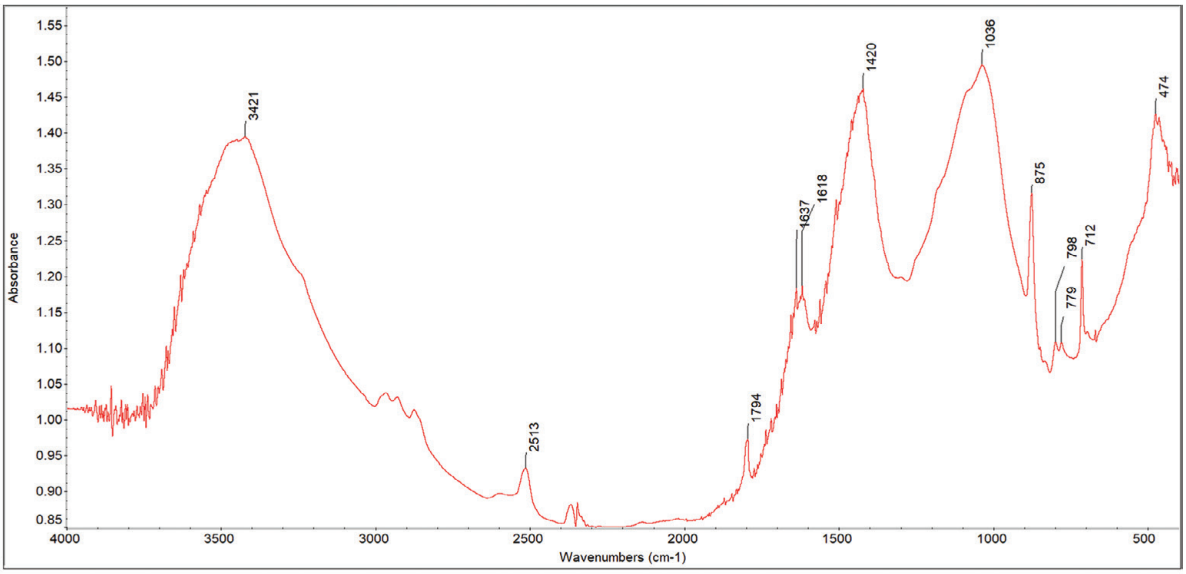

13

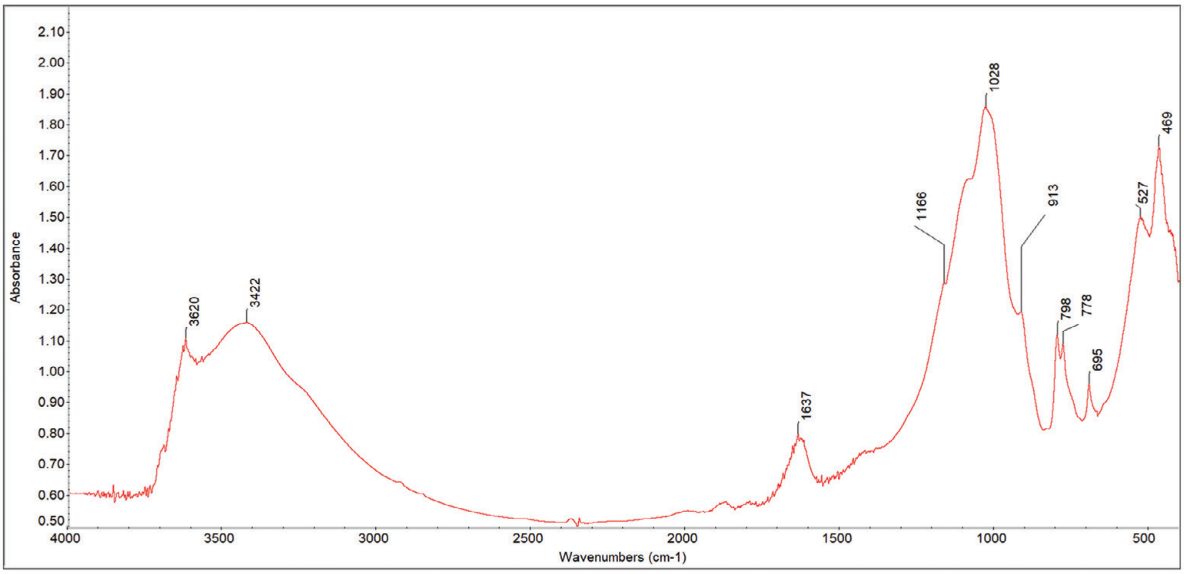

14

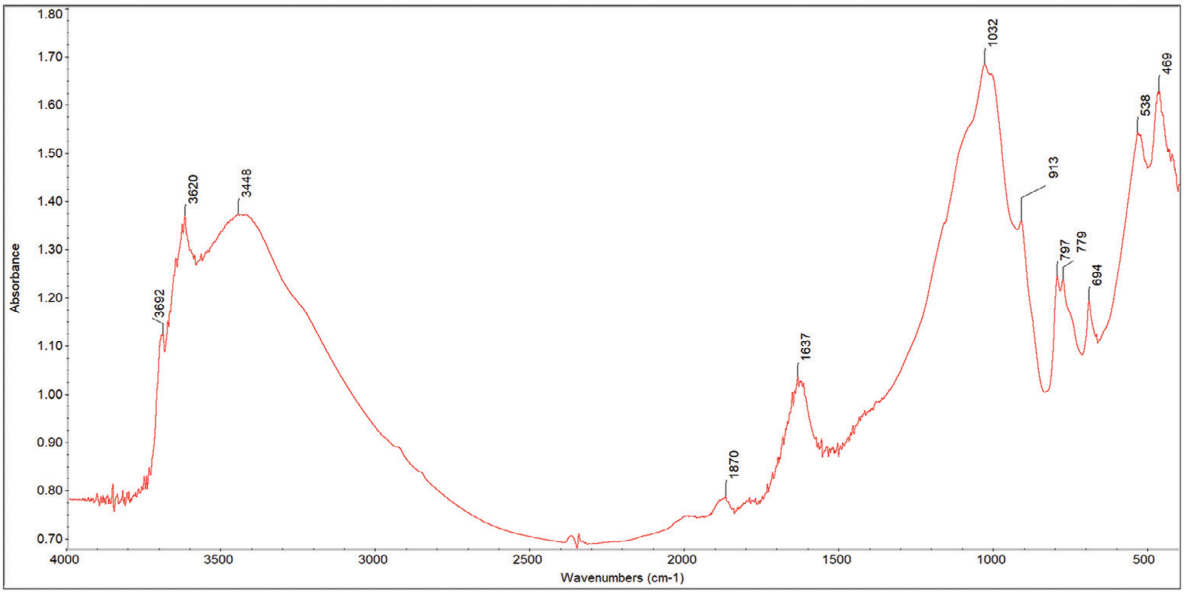

15

Appendix 6

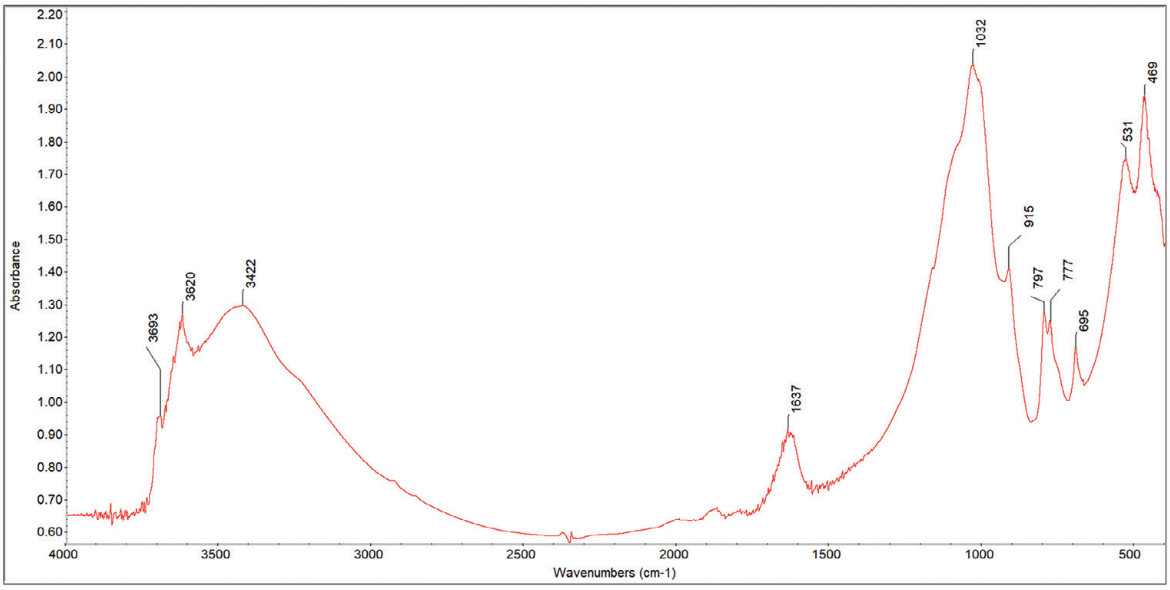

16

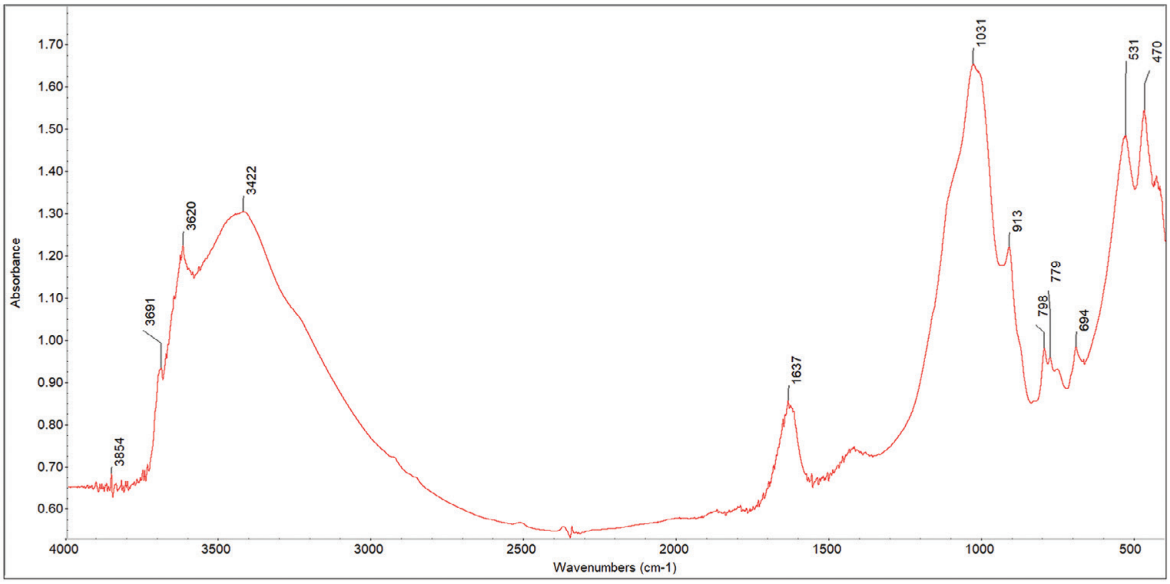

17

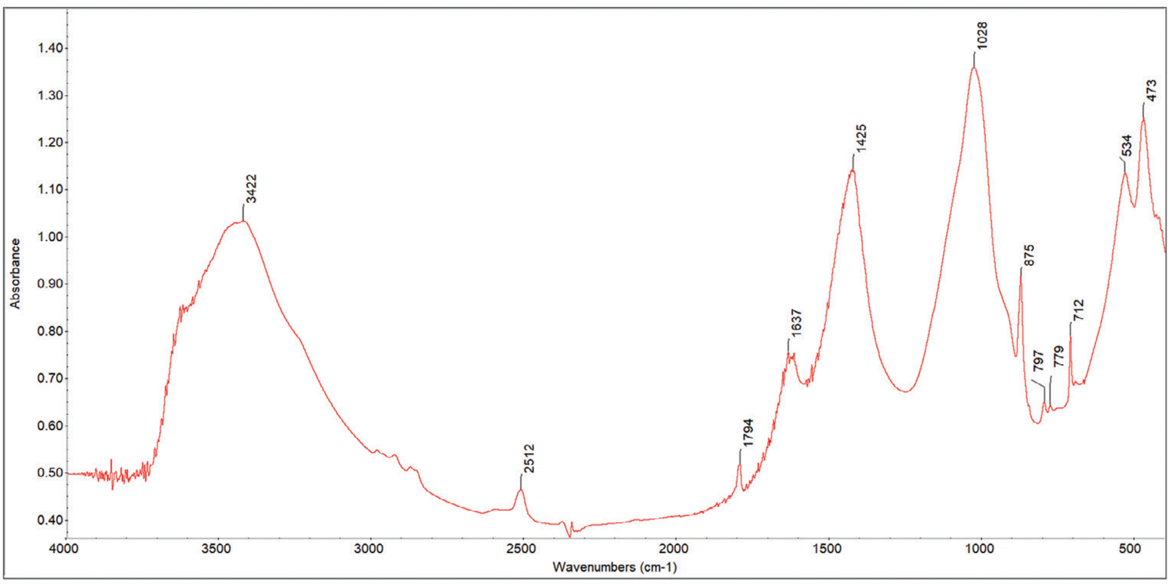

18

Appendix 7

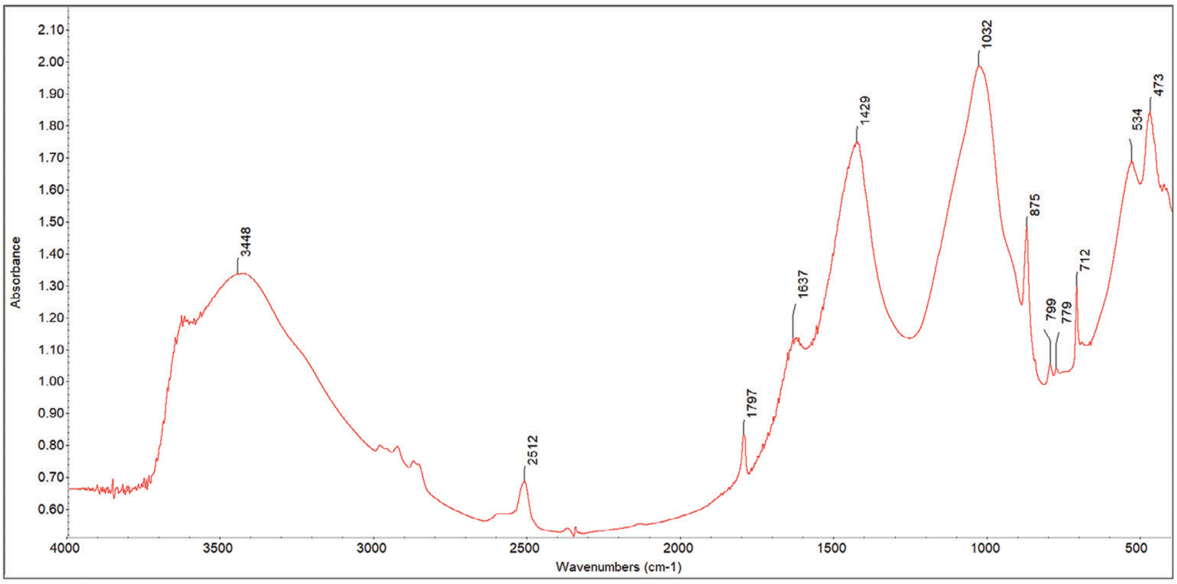

19

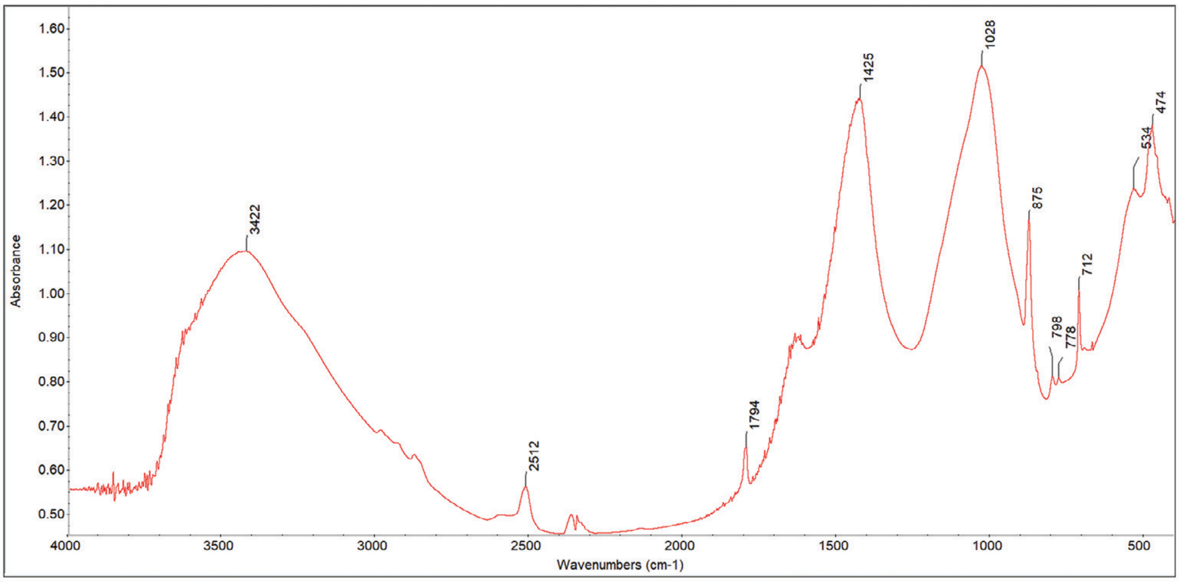

20

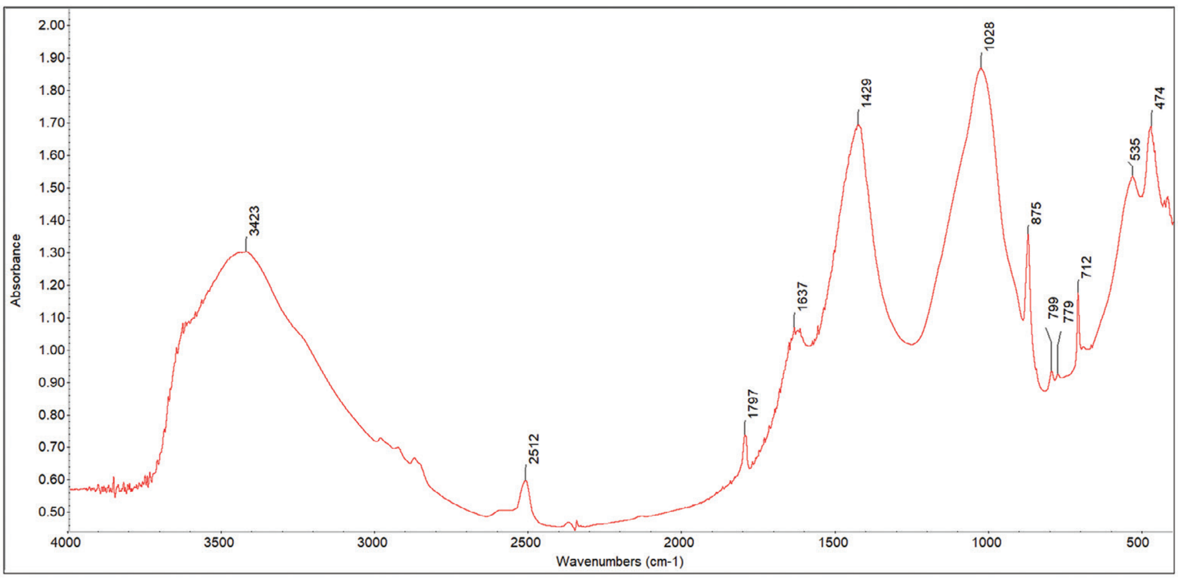

21